Natural Resources Canada | Ressources naturelles Canada

GEOLOGICAL SURVEY OF CANADA
OPEN FILE 7390

Technical Guidelines for Reduction of Space Weather Impacts on Geostationary Satellites

H.-L. Lam

2015

Canada

GEOLOGICAL SURVEY OF CANADA
OPEN FILE 7390

Technical Guidelines for Reduction of Space Weather Impacts on Geostationary Satellites

H.-L. Lam

Geomagnetic Laboratory, Geological Survey of Canada, Natural Resources Canada, 2617 Anderson Road, Ottawa.

2015

doi:10.4095/295685

This publication is available for free download through GEOSCAN (http://geoscan.nrcan.gc.ca/).

Recommended citation
Lam, H.-L., 2015. Technical Guidelines for Reduction of Space Weather Impacts on Geostationary Satellites; Geological Survey of Canada, Open File 7390, 72 p. doi:10.4095/295685

Publications in this series have not been edited; they are released as submitted by the author.

Contents

Abstract

An overview of space weather effects on geostationary satellites and engineering designs to lessen such effects is first presented. Guidelines related to NRCan Space Weather Group's work on the reduction of space weather impact on geosynchronous satellites then follow. It is shown that NRCan's real-time geomagnetic data can be utilized to provide warning and situational awareness of possible surface charging of satellites. Daily forecasts of energetic electron fluence by the Space Weather group can forewarn of dangerously high electron levels that signal possible internal charging of satellites up to three days in advance. Thus, NRCan's real-time geomagnetic data and electron forecasts provide guidelines for satellite operators to take appropriate actions to alleviate the space weather impact on their satellites. A Space Weather Anomaly Investigation System to discern space environmental causes of satellite operational anomalies has been developed so that the anomaly history of a particular satellite due to specific space weather condition can be chronicled for consideration in future design modification of satellites of similar make for the mitigation of space weather impacts.

Introduction

In 2000, the total insured values of the 254 insured satellites in orbit was $21 billion, while the total value of the more than 600 satellites in orbit was $50-100 billion [Kunstadter, 2000]. Thus, the satellite enterprise represents huge assets of human built structures. From 1994 to 1999, a total of $3.8 billion in insured losses was incurred, with 22 total losses and 91 partial losses. The causes of the losses were due to commercial pressures, new launch vehicles, and space environment. Space weather was suggested as a cause contributor to over $500 million in satellite insurance claims for the same period. Separately, the U.S. Department of Defense has estimated that disruptions to government satellites from space weather cost about $100 million a year [Rodgers, et. al., 2000]. While figures for recent years are not available, the above sample has given a good indication of the economic impact of space weather on satellite industry. Besides total or partial satellite losses, numerous cases of reduction in satellite capability, loss of component redundancy, and other satellite operational anomalies, which are nuisances to satellite operators, were also the result of space weather.

Satellite malfunctions not only pose economic losses to the industry, but also severely impact society, as exemplified by the failures of Anik-E1 and E2 satellites on January 20, 1994 [Lam et al., 2012]. The outages of the Anik-Es wreaked havoc with television, computer data transmissions across Canada and phone services to northern communities for hours. To alleviate the space weather impacts on satellites, designs engineered to withstand the adverse space weather conditions as well as forecasts and situational awareness of the disturbed space environment should be considered. This

document will dwell into both the design and space weather considerations, after describing the space weather effects on geostationary satellites.

Radiation Belts

The region of space where satellites traverse consists of two doughnut-shaped belts, the inner radiation belt and the outer radiation belt, where energetic electrons and protons are magnetically trapped, gyrating and bouncing along field lines as well as drifting across them (Fig. 1). The environment of the belts is highly dynamic both temporally and spatially, as revealed by observations. The disturbed space weather conditions in the radiation belts constitute a hazard to space activities for spacecrafts in a range of orbits, including the all important geostationary orbits of communication satellites. Mitigation measures that need to be taken would require a predictive knowledge and situational awareness of that hostile space environment.

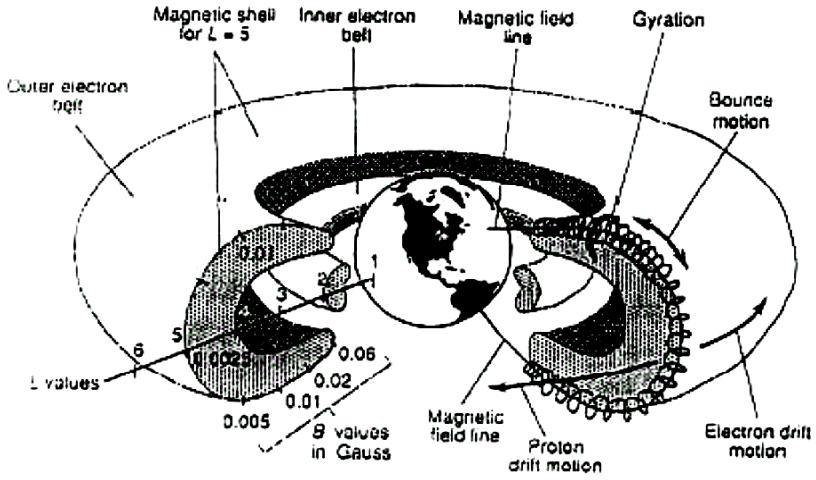

Fig. 1. Doughnut-shaped inner and outer radiation belts

The inner belt, extending from roughly 1.1 to 3.5 Earth radii (R_E), is populated by protons in the 10-100 MeV range, which readily penetrate spacecraft, as well as electrons in the range of hundreds of keV. The outer belt, extending from about 3 to 7 R_E with greatest intensity around 4-6 R_E, consists mainly of electrons in the 0.1-10 MeV range. The outer belt is larger than the inner belt, and is characterized by highly variable fluxes of energetic electrons. A cross-section of both belts is shown in Fig. 2.

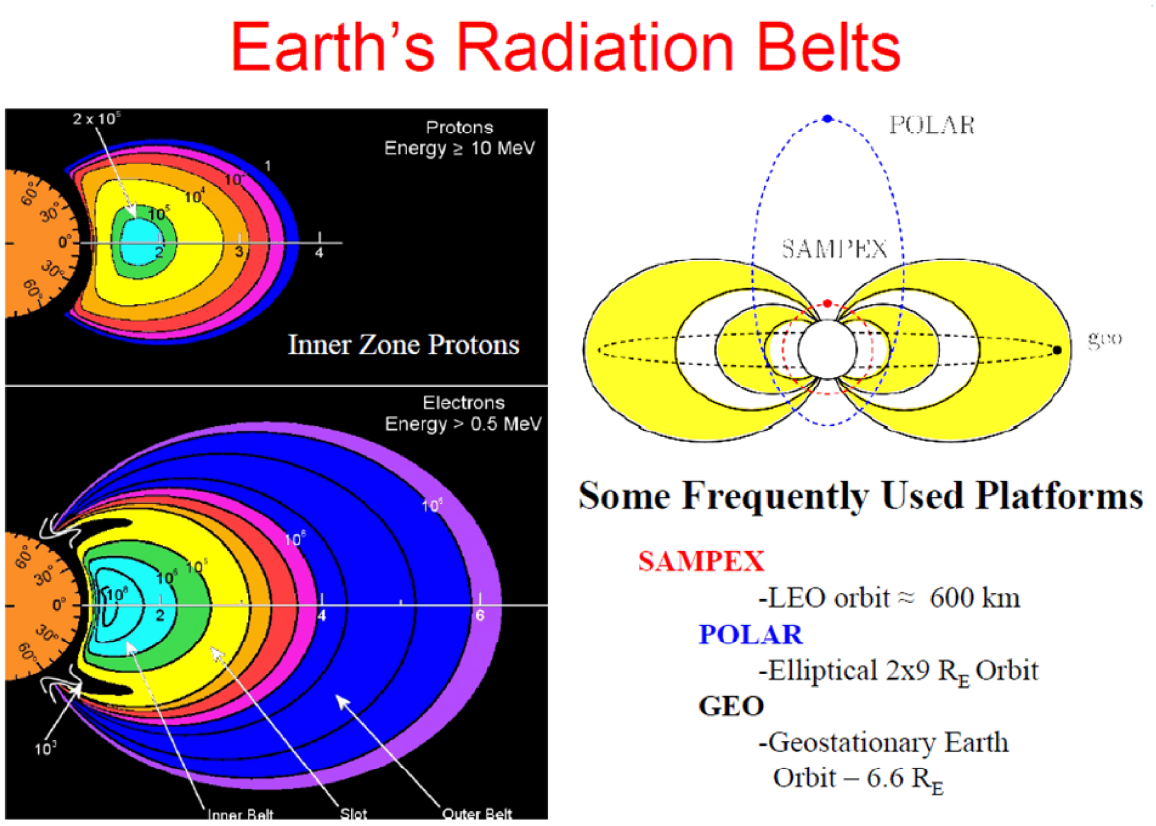

Fig. 2. Cross-sections of inner and outer radiation belts (left) and the satellite orbits with respect to the radiation belts (right).

Fig. 2 also displays the satellite orbits with respect to the radiation belts. They are the low Earth orbit (LEO) as represented by SAMPEX, the elliptical orbit as represented by POLAR, and the geostationary orbit as represented by GEO. An equatorial view of the above orbits together with meduim Earth orbit (MEO) and semi-synchronous orbit is shown in Fig. 3.

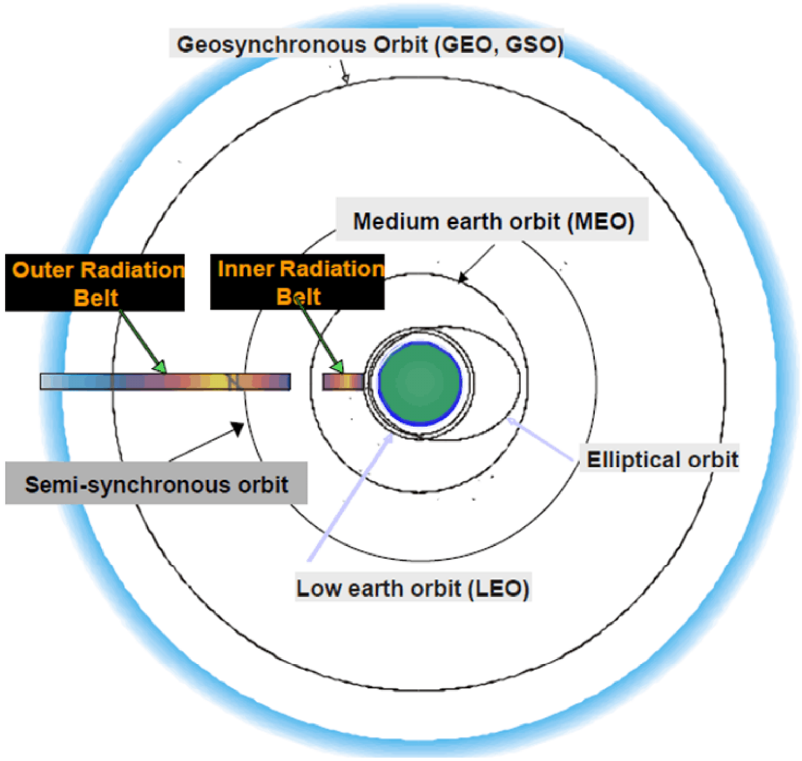

Fig. 3. Satellite orbits on equatorial plane.

This document is concerned with satellites in geosynchronous orbit at 6.6 R_E, which, though located just beyond the region of high concentration of electron fluxes of the outer radiation belt, is nonetheless often subjected to bombardment by high fluxes of energetic electrons.

Space Environment Effect

Geosynchronous satellites are operating in a space environment that is populated with charged particles. These particles can affect satellites in a variety of ways, either directly by penetrating into the satellite electronics [as shown by (a) single Event Upset in Fig. 4 (after Allen, 2002)], or indirectly through spacecraft charging [as shown by (b) Deep-Dielectric Charging and (c) Surface Charging in Fig. 4] , with the resulting electrostatic discharge that could cause problems. These direct or indirect processes can result in satellite operational anomalies such as phantom commands, random part failures, damage to electronics, loss of control, and even satellite failure.

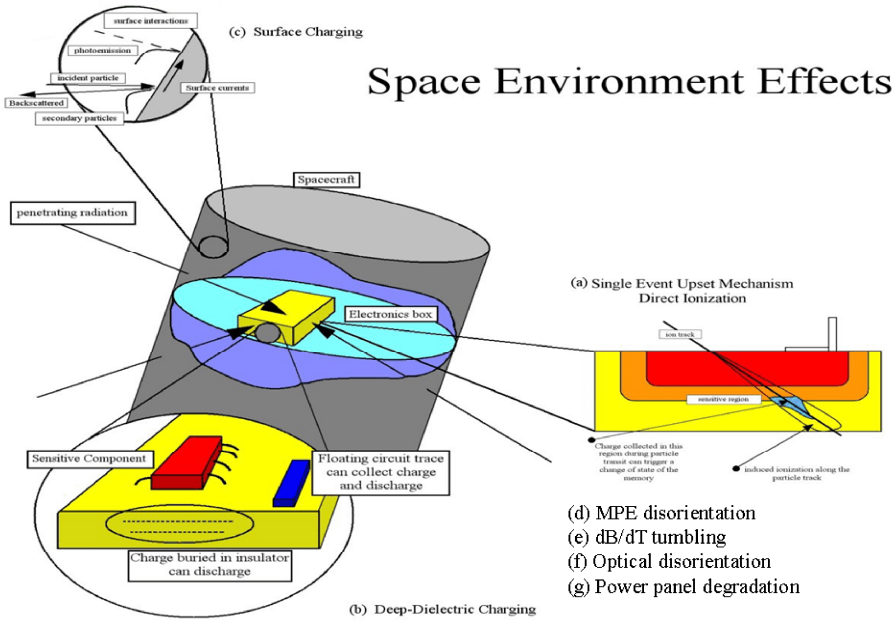

Fig. 4. Space environment effects on satellites.

The geostationary orbit is a circular orbit (see Fig. 3) immersed in a space environment that is dominated by energetic electrons (see Fig. 2). This environment is characterized by strong temporal variations of electrons with many extended quiet periods of low electron flux interspersed by episodes of intense injections of energetic electrons which increase the prospect of spacecraft charging. Also, solar protons and cosmic rays have unrestricted access to this orbit. Solar particles, though not directly participating in charging process, make short-lived but important contribution to single event upsets while cosmic rays can provide a continuous source of single event effects. Thus, (a) Single Event Upset, (b) Deep-Dielectric Charging, and (c) Surface Charging are the most important "space environment effects" amongst others listed in Fig. 4, and they will be highlighted separately below.

Single Event Upset

When very high energy protons or heavier nuclei plough through semiconductor devices, they produce a large number of electrons and holes that carry currents within these devices (Fig. 5). Large numbers of electron-hole pairs introduced into sensitive regions like memory cells can alter information, and result in phantom commands. Effects can be devastating if ion impacts occur in control systems or decision-making circuits. In addition, these impacts degrade semiconductor lifetimes.

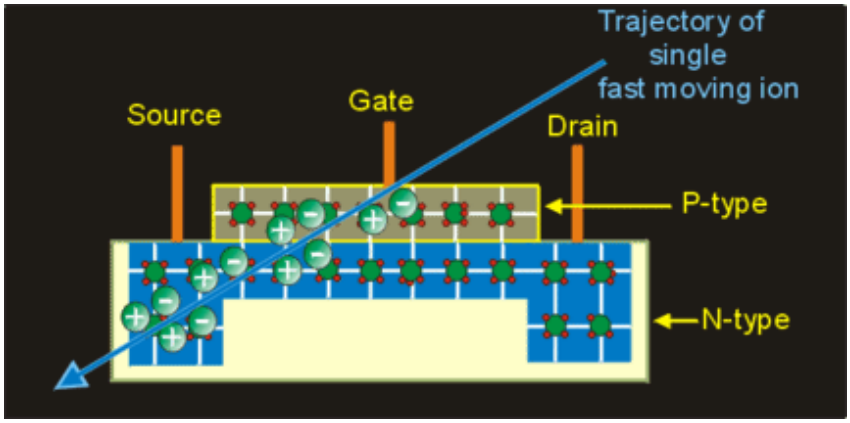

Fig. 5. SEU caused by penetrating energetic ions.

The direct circuit penetration of such high energy particles can be the result of bombardment of the satellite by energetic protons. NOAA's Space Weather Prediction Center (SWPC)

(http://www.swpc.noaa.gov) declares “Proton Events” when the particle flux of > 10 MeV protons exceeds a threshold. An example of proton events is shown in Fig. 6 (after Allen, 2000) where I1, I2, I3, I4, I5, I6, I7 refer to protons in Mev energy range of 0.6-4.2, 4.2-8.7, 8.7-14.5, 15.0-44.0, 39.0-82.0, 84.0-200.0, and 110.0-500.0 respectively.

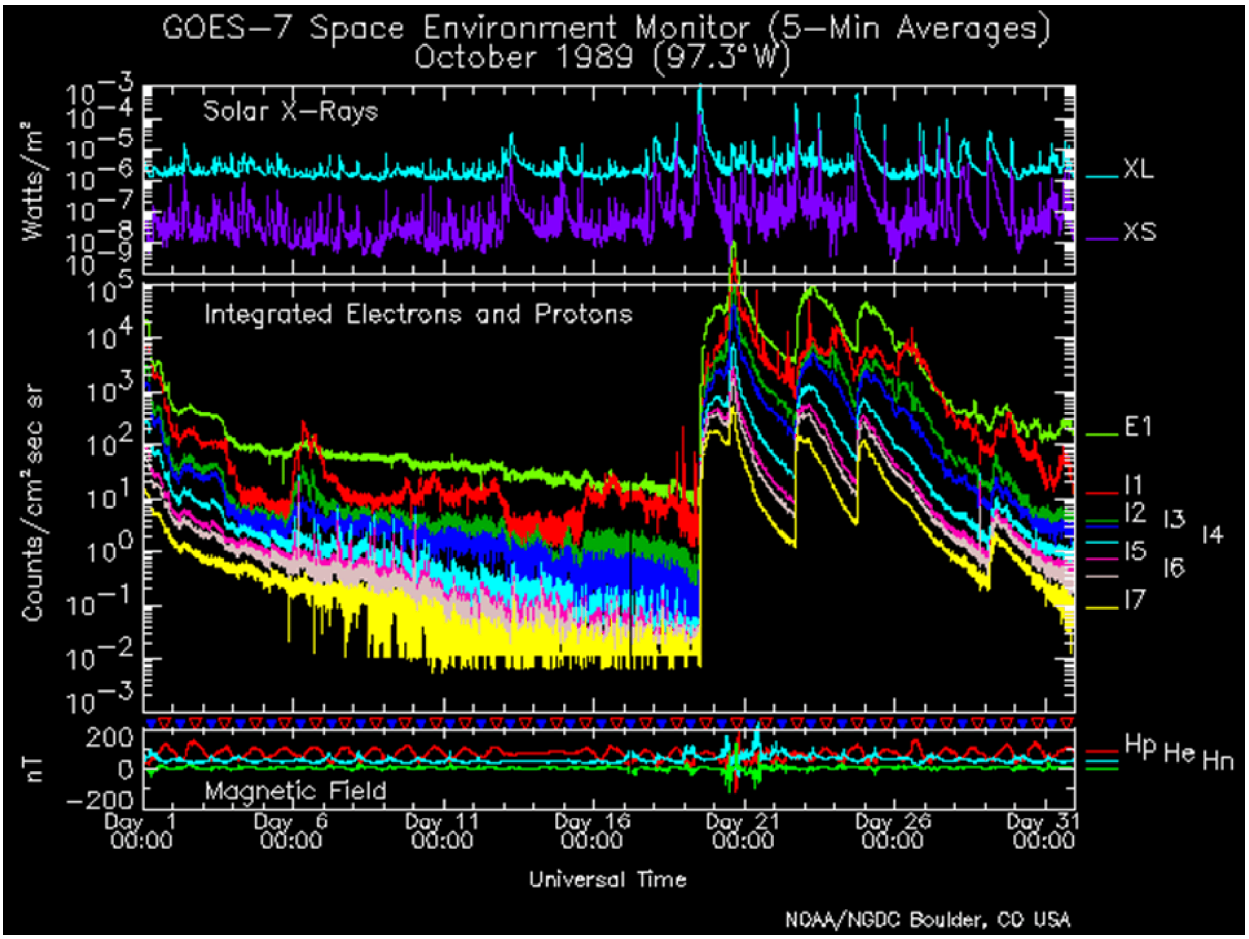

Fig. 6. Example of proton events.

During large proton events, energetic protons burn tracks through chips and cause upsets of memory. An example of SEU due to a proton event is shown in Fig. 7 (after Allen, 2000) showing upsets in memory in TDRS-1 satellite during a major proton event.

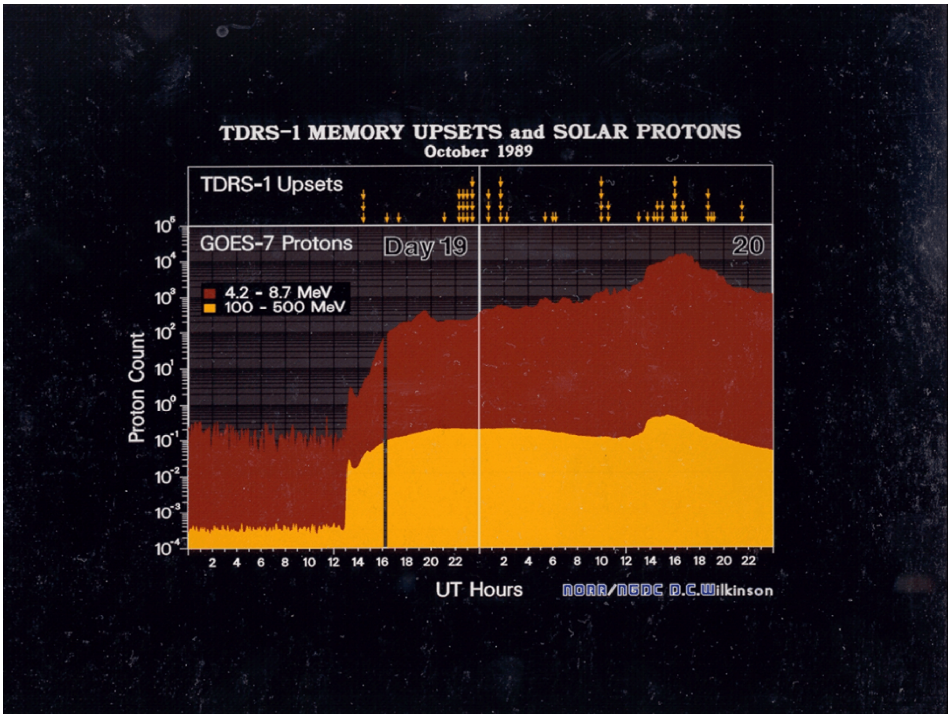

Fig. 7. SEU and proton event.

SEUs arising from high energy protons and heavier nuclei are due to their direct penetration through the satellite whereas satellite operational anomalies caused by spacecraft charging, whether it be surface or deep-dielectric, are due to arcing after charge build-up. Thus, different space weather conditions would

have different space weather impacts on satellites, with proton events giving rise to SEUs, and with occurrences of substorms and episodes of very high energy electrons causing surface and internal spacecraft charging respectively, as shown below.

Surface Charging

Positive charging of a satellite can occur as illumination of the spacecraft surface by photons knocks off the loose electrons. As these electrons are freed from the spacecraft by photoemission, the satellite develops a relative positive charge. Negative charging of a satellite in geosynchronous orbit can also occur due to electron bombardment. Incidence of a large incoming flux of electrons in the absence of sufficient charge drainage by mechanisms such as photoemission can result in large negative potentials. Indeed, large negative potentials in the mutlikilovolt range were observed in geostationary satellites as early as 1972 [DeForest, 1972]. If the entire surface of the satellite were a homogeneous conductor, the charge buildup on the surface would generate a current flow to spread the charge evenly over the satellite. Thus, absolute charging of a spacecraft with respect to the ambient plasma does not pose serious problems. However, since there is marked difference in conductivity across the satellite surface because most spacecraft exteriors have solar panels, probes, lenses, etc., differential charging of the satellite may result. Differential charging can induce electrostatic discharges that could result in anomalous behaviors of geostationary satellites. Satellite operational anomalies attributable to differential surface charging were well documented decades ago [e.g. Rosen, 1976; Garrett and Pike, 1980], and the subject has since received much attention.

Geosynchronous satellites are susceptible to electron bombardment associated with magnetospheric substorm, which is a sudden and dynamic energy release process on the night side of the Earth. The

ground magnetic signature of magnetospheric substorm is magnetic substorm. For simplicity, the term substorm will be used. It has long been established that substorms in the midnight sector are responsible to satellite operational anomalies due to surface charging [e.g. Rosen, 1976; Steven and Pike, 1981], as evidenced in the local time distribution of satellite operational anomalies in the very early 70's around solar maximum shown in Fig. 8 (after McPherson et al., 1975). It can be seen from the figure that there is a cluster of satellite anomalies in the midnight to dawn sector. During substorms, streams of hot electrons (1- 80 keV) are injected earthward from the magnetotail around local midnight, drift eastward from midnight to dawn, and then encounter the satellites in geostationary orbit, causing surface charging. The resultant discharge due to differential surface charging would then lead to the occurrences of satellite operational anomalies in the midnight to dawn sector, as shown in Fig. 8.

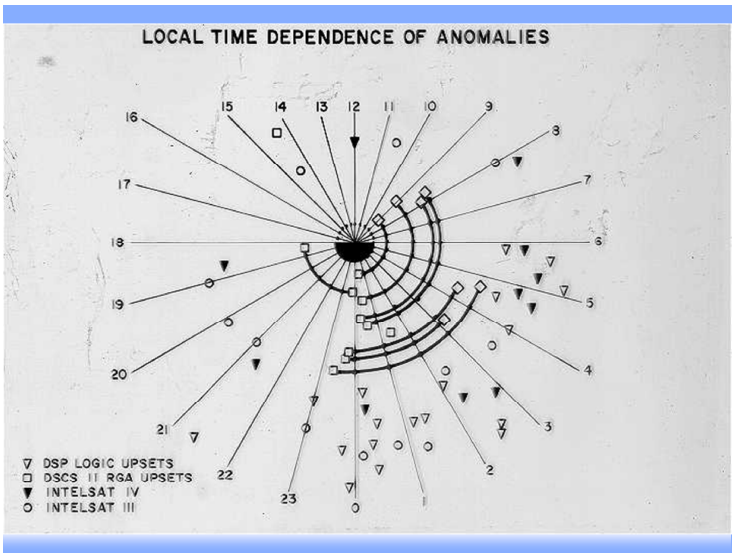

Fig. 8. Local time distribution of occurrences of satellite operational anomalies.

Internal Charging

In contrast to the lower energy hot electrons that only charge up the surface of a satellite, energetic electrons with energies > 2 MeV can penetrate the surface of a satellite and deposit charges within the bulk of dielectric materials or on the surface of isolated conducting material interior of the spacecraft. Such charging process is known as deep dielectric charging, as shown earlier in the diagram of Allen [2002] (Fig. 4), or bulk charging or buried charge process or simply internal charging. This concept of buried charge was proposed early on in the mid 70's by Meulenberg [1976]. However, back in the 70's and 80's the impact of the energetic electrons at geostationary altitude was not fully appreciated. Substorms and surface charging events were of primary concern then. However, it has now become abundantly clear that internal charging plays a significant role in causing satellite operational anomalies, as conclusively demonstrated by Wrenn [1995]. The January 1994 Telesat Canada's Anik-E1 and E-2 failures that wreaked havoc in communication across Canada were no exceptions, with internal charging by energetic electrons being the culprit [Baker et al., 1994; Lam et al., 2012].

Since a geostationary satellite is located at 6.6 R_E at the fringes of the outer radiation belt (see Fig. 2), just beyond the intense energetic electron region, the satellite is generally safe from internal charging by energetic electrons. However, fluxes of >2 MeV energetic electrons at geostationary orbit as measured by NOAA's GOES geosynchronous satellites can sometimes be much enhanced, posing a dangerous situations for satellites. An example of the large variability of energetic electron flux at geosynchronous

orbit is shown in Fig. 9 (from NOAA's Space Weather Prediction Center (SWPC) web site: http://www.swpc.noaa.gov/ftpdir/plots/electron/20100313_electron.gif).

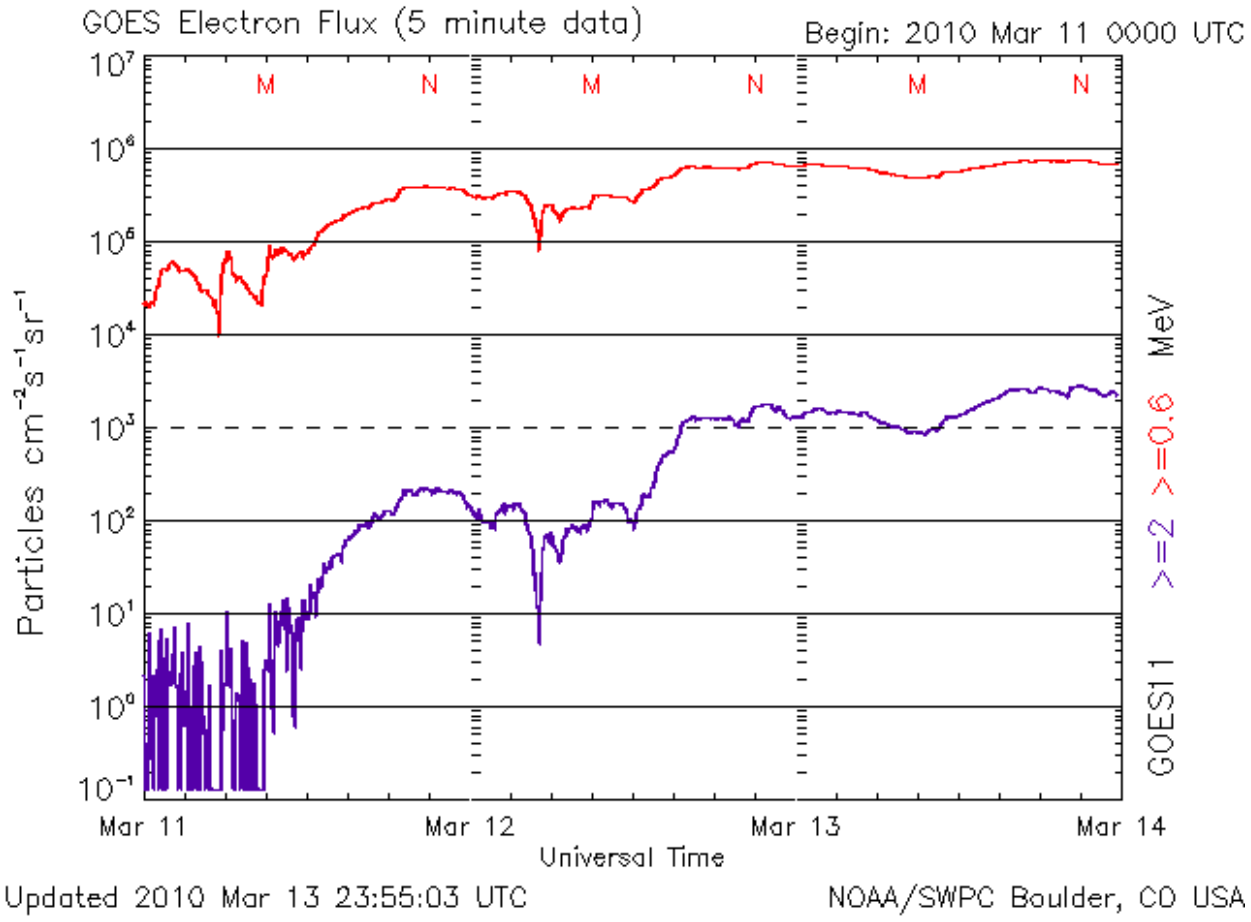

Fig. 9. An example of >2 MeV electron flux variations at geosynchronous orbit.

Fig. 9 shows that >2 MeV electron flux (blue line) as measured by GOES 11 geosynchronous satellite varied from very low flux on March 11 to very high flux on March 13 after crossing the dashed line at 10^3 flux level which NOAA/SWPC designates as threshold for high flux.

The high particle flux conditions are often associated with the co-rotating high-speed solar wind streams emerging from large solar coronal holes, which occur often during the descending phase of a solar cycle. Thus, periods of enhanced energetic electrons are most common during the declining years of the sunspot cycle, as shown in Fig. 10 (after Lam, 2004), which shows the yearly values of > 2MeV electron fluence (flux accumulation over 24 hours) and DRX (a daily magnetic index that is the average of 24 hourly ranges in the X component of the geomagnetic field measured in the auroral zone) from 1987 to 1997, with Solar Cycle 22 curve superimposed. The figure clearly indicates low energetic electron fluence around solar maximum and high electron fluence during the descending phase of the solar cycle. Also worthy of note are the magnetic activity peaks that occur not only around solar maximum when eruptive solar events prevail but also during the declining phase of the solar cycle when co-rotating coronal holes are persistent solar features.

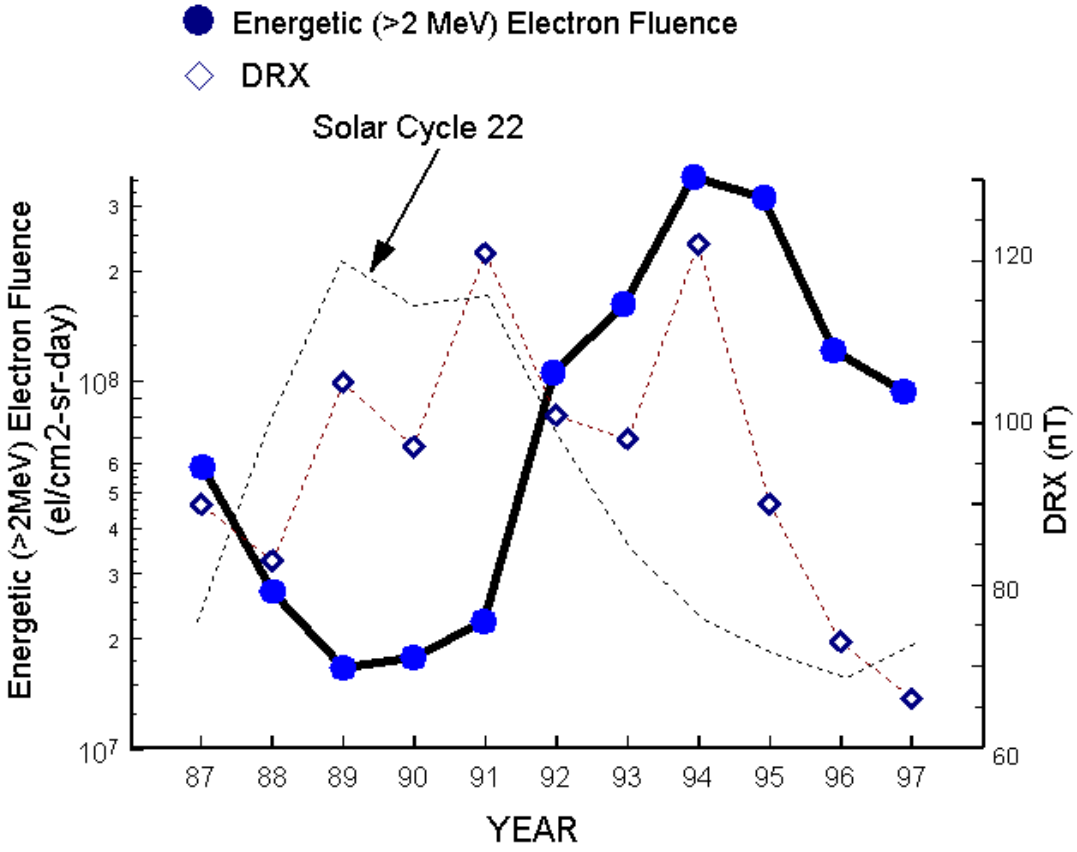

Fig. 10. Yearly variations of energetic electrons fluence and geomagnetic activity in a solar cycle.

Fig. 11 (after Lam and Hruska, 1991) shows the local time dependence of 122 well-documented satellite operational anomalies (from a proprietary source) experienced by a single communication satellite at geostationary orbit from April 1983 to December 1987 during the descending phase of a solar cycle.

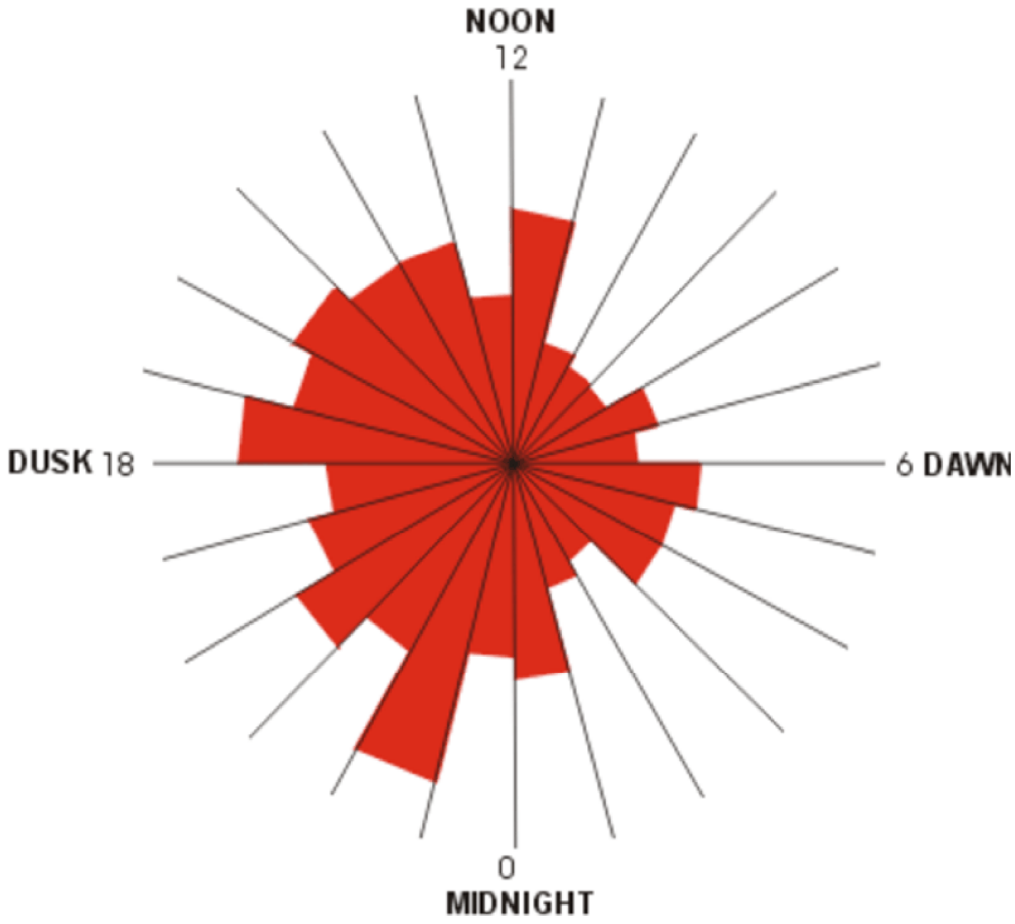

Fig. 11. Local time distribution of occurrences of satellite operational anomalies based on 122 reported events from a single geosynchronous satellite.

A comparison of the above figure with Fig. 8 shows that it displays a different local time pattern. Whereas Fig. 8 indicates that the majority of satellite anomalies occurred in the local time sector from midnight to dawn, Fig. 11 shows that most anomalies appeared in the afternoon and evening sector. The discrepancy may be related to the fact that Fig. 8 was based on several satellites and that Fig. 11 was derived from one single satellite with more events. However, a better explanation can be found in Fig. 10, which shows anti-correlation between energetic electrons and solar cycle. Thus, based on this relationship, internal charging was unlikely to be the cause of the anomalies of Fig. 8 as the events occurred around solar maximum with few energetic electrons, while internal charging was highly likely to be responsible for the majority of the anomalies in Fig. 11, as the incidents occurred during the declining phase of a solar cycle with more energetic electrons. Although it may be difficult, without particle data and proprietary information from satellite operators, to differentiate between anomalies due to differential surface charging and those due to internal charging as the telemetered data signature is also similar, however, based on the above argument and to a first approximation, Fig. 8 can be considered as the local time distribution of anomalies due to differential surface charging by hot substorm electrons whereas Fig. 11 can be considered as the local time dependence of anomalies due to internal charging by penetration of energetic electrons. It is thus of interest to note that the malfunctions of the 1994 Telesat Canada's Anik-E1 and E-2, which have been shown to be due to internal charging by energetic electrons, occurred at 1734 UT on January 20 and 0214 UT on January 21 approximately around noon and dusk in satellite local time [Lam et al., 2012] in conformity with the pattern shown in Fig. 11. The large number of anomalies in the 22-23 LT interval is worth noting because the interval coincides with the location of the Harang discontinuity [Heppner, 1972], which is a transition region in

the polarity of the ionospheric electric field in the auroral oval. During substorms the discontinuity becomes quite dynamic with auroral arcs brightening and net field aligned current diverging upward. Fig. 11 suggests that the inflowing substorm electrons associated with these phenomena encountered the satellite, charging up the surface differentially with the resultant anomalies.

Reduction of Space Weather Impacts

Design Consideration

The NASA particle models of AP-8 [Sawyer and Vette, 1976] and AE-8 [Vette, 1991] have a long history of driving the selection of parts and the design of shielding for satellites, as these models, based on compiled data from many satellites, remain the standard for specifying protons and electrons environment respectively in the radiation belts (Fig. 12). The models were developed at Aerospace Corporation for NSSDC at NASA/GSFC based on data from satellites flown in the 1960s and early 1970s. They provide estimates of the omnidirectional fluxes of protons in the energy range of ~50 keV to 500 MeV and electrons in the energy range of ~50 keV to ~7 MeV.

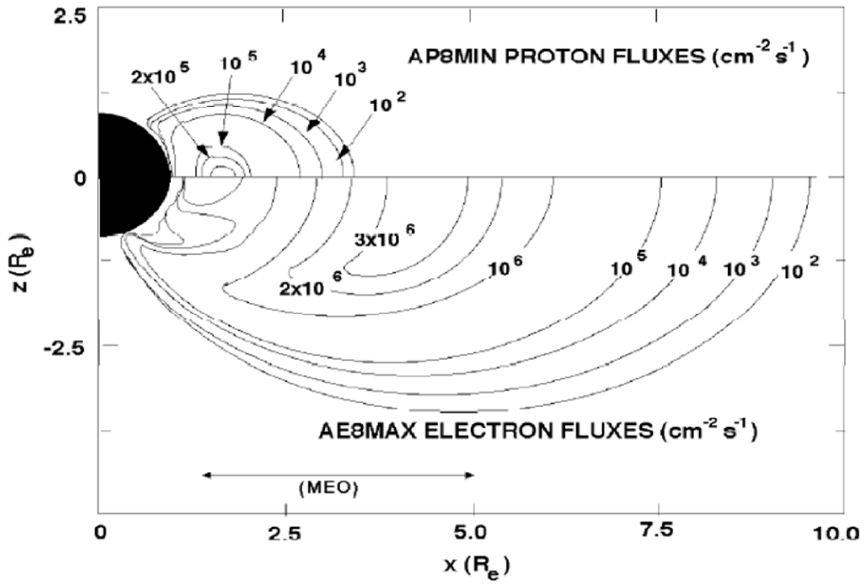

Fig. 12. Schematics of the Earth's radiation belts as estimated by the AE-8 and AP-8 models.

With AE-8 and AP-8 models based only on average values of particle fluxes without inclusion of time-dependent variations of the radiation fluxes such as those due to geomagnetic storms, better definitions for worst-case scenarios are needed in satellite design to avoid space environmental effects on the satellites. There are the two complementary NASA documents which provide design guidelines for such purpose. These two documents are: NASA-TP-2361 entitled "Design Guidelines for Assessing and Controlling Spacecraft Charging Effects" [Purvis et al., 1984], and NASA-HDBK-4002 entitled "Avoiding Problems Caused by Spacecraft On-Orbit Internal Charging Effects" [Mulville, 1999]. They are standard handbooks for mitigating charging effects by design to reduce the risks of satellite operational anomalies due to surface and internal charging. Since errors in estimating the radiation environment can result in substantial economic impact through excessive shielding or early satellite loss, it is critical from the start to have access to the best estimates of the radiation environment.

Fig. 13 (after NASA-HDBK-4002 [Mulville, 1999]) shows a comparison between the often used NASA AE8min electron spectrum and the worst-case electron integral spectrum at geosynchronous orbit, that was derived using data from SOPA and ESP instruments of the Los Alamos LANL satellite for high environment days gauged by GOES >2 MeV electron data. As can be seen, the AE8min spectrum, designed to be a long-term average, is substantially lower, and is inadequate for use to avoid internal charging. The figure clearly shows large difference between the nominal time averaged (AE8) and shorter-term "worst-case" conditions, which is characteristic of Earth's radiation environment.

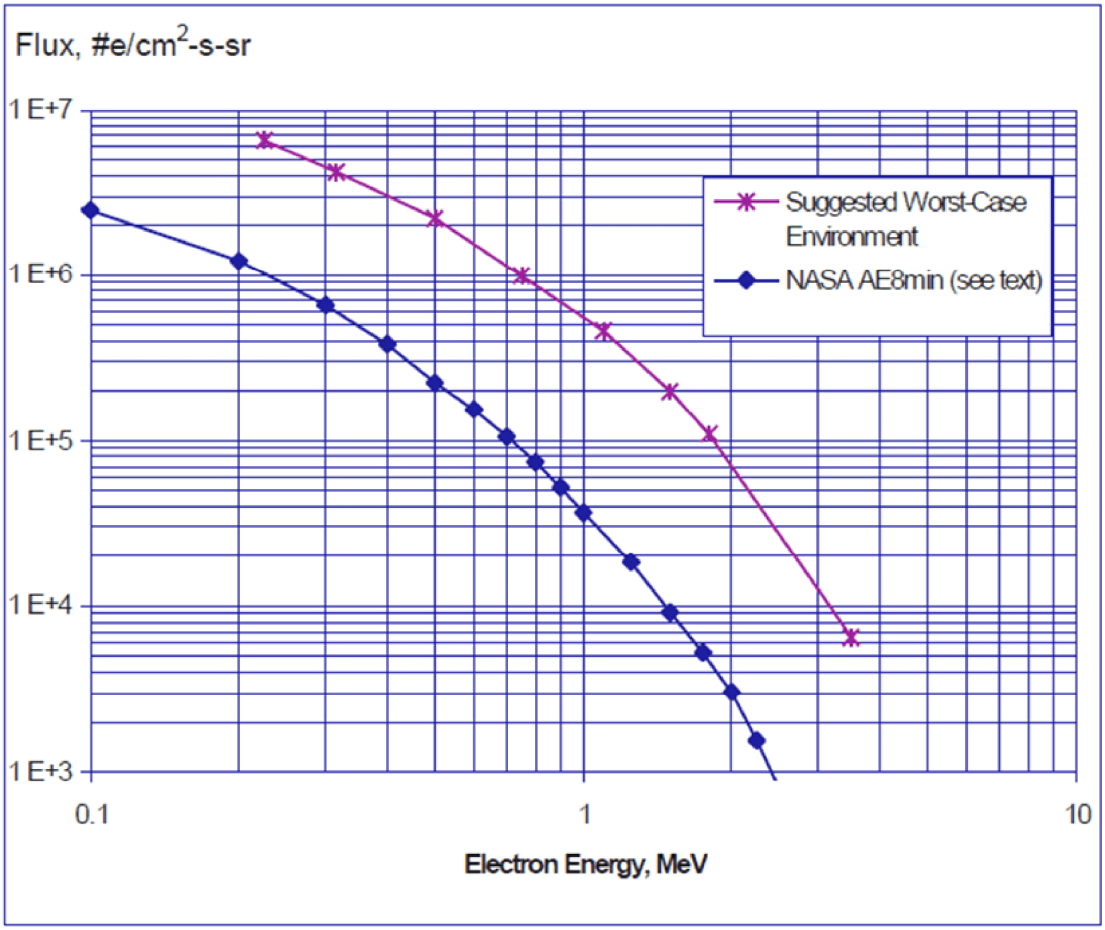

Fig. 13. Electron flux spectrum at geosynchronous orbit for worst-case short-term environment (upper) and NASA AE8min long-term average environment (lower) from NASA- HDBK-4002.

As a case in point, the particle environment generally specified by Telesat Canada for its geosynchronous satellites is based on the values indicated in Table 1 of NASA-TP-2361 scaled to 99th percentile [Gubby and Evans, 2002]. The NASA Table is reproduced below in Fig. 14 (after NASA-TP-2361 [Purvis et al., 1984]).

TABLE I. - WORST-CASE GEOSYNCHRONOUS PLASMA ENVIRONMENT

Electron number density, N_E, cm^{-3}	1.12
Electron temperature, T_E, eV	1.2×10^4
Ion number density, N_I, cm^{-3}	2.36×10^{-1}
Ion temperature, T_I, eV	2.95×10^4

Fig. 14. Worst-case electron environment spec from NASA-TP-2361 .

Fig. 15 (after NASA-HDBK-4002 [Mulville, 1999]) shows depth of penetration into aluminum vs energy of electrons and protons. This gives the satellite's shielding thickness required to prevent particle with specific energy from penetrating into the spacecraft interior. If the material is not aluminum, an equivalent penetration depth can be approximated by substituting an equivalent number of grams per square centimeter of thickness.

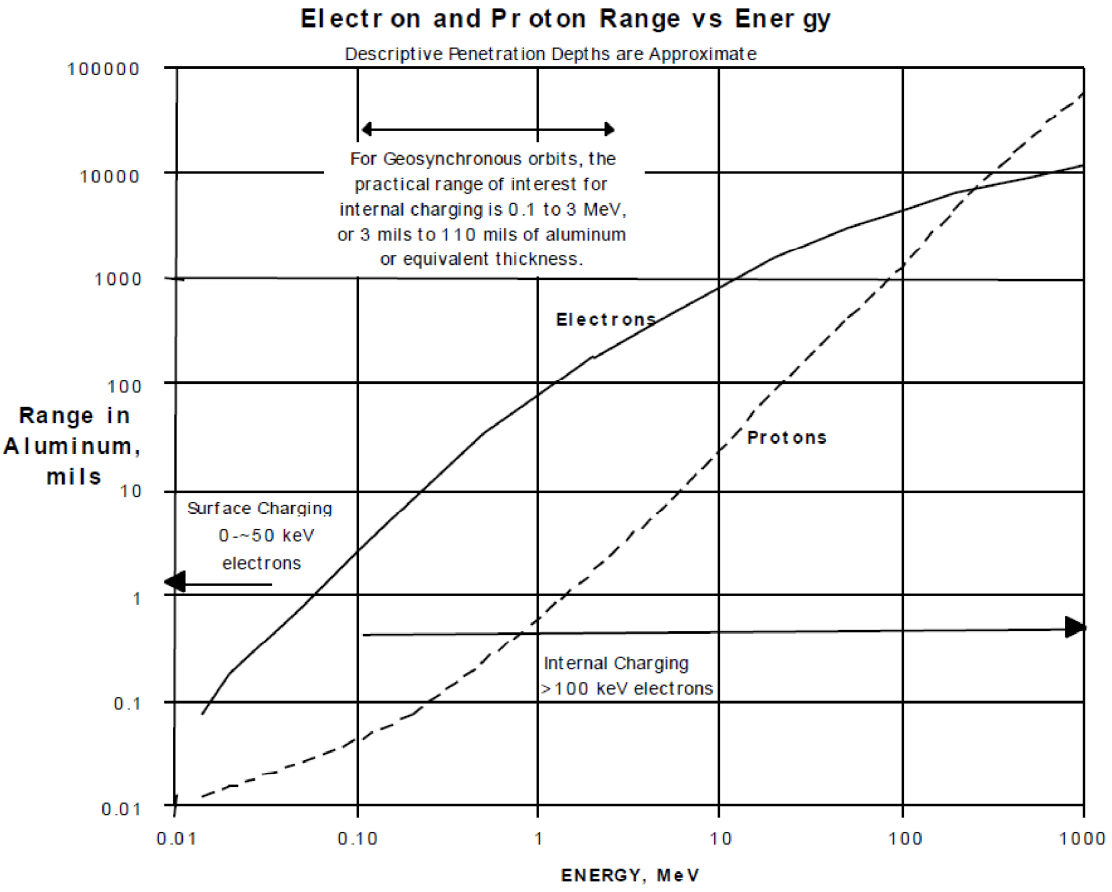

Fig. 15 Penetration depths in aluminum by electron/proton from NASA-HDBK-4002.

From Fig. 15, it can be seen that at least 110 mils of aluminum or equivalent thickness is required to stop the >2 MeV electrons from getting inside the satellite. For single event upset (SEU), increasing shielding to prevent the penetration of heavy ions may not be effective. Adams [1981] showed that shielding of 20 g/cm^2 only reduces particle flux by less than a factor of 10 compared to the standard satellite shielding of 2 g/cm^2 provided by a typical skin and electronic box. Besides, the weight and volume of 20 g/cm^2 with 3.0 inches of aluminum is not a reasonable solution. There may be other methods for use on satellite electronics to mitigate the impact of SEUs. For example, avoiding the problem through parts selection may be feasible. Also, memory redundancy may provide a high degree of fault tolerance from part failure. Of course, there are negative factors such as additional weight and power required for the additional memory. Thus, satellite designers must evaluate these methods in order to trade off the penalties, and develop a protection scheme while still meeting the system requirements.

Fig. 16 (after Farthing et al., 1982) demonstrates changes in anomaly occurrences with respect to magnetic activity after the history of GOES-4 were incorporated into designing GOES-5. The plot indicates that as the Kp magnetic activity index increased, the GOES-4 anomaly relative frequency rate rose exponentially. However, after design changes were made in GOES-5, with rising magnetic activity, GOES-5 anomalies increased at only a linear rate, rather than a non-linear rate as in GOES-4. Thus, engineering modifications made on GOES-5 after consideration of the earlier GOES-4 data resulted in the reduction of sensitivity to lower energy electrons by GOES-5, though the effect was not completely removed.

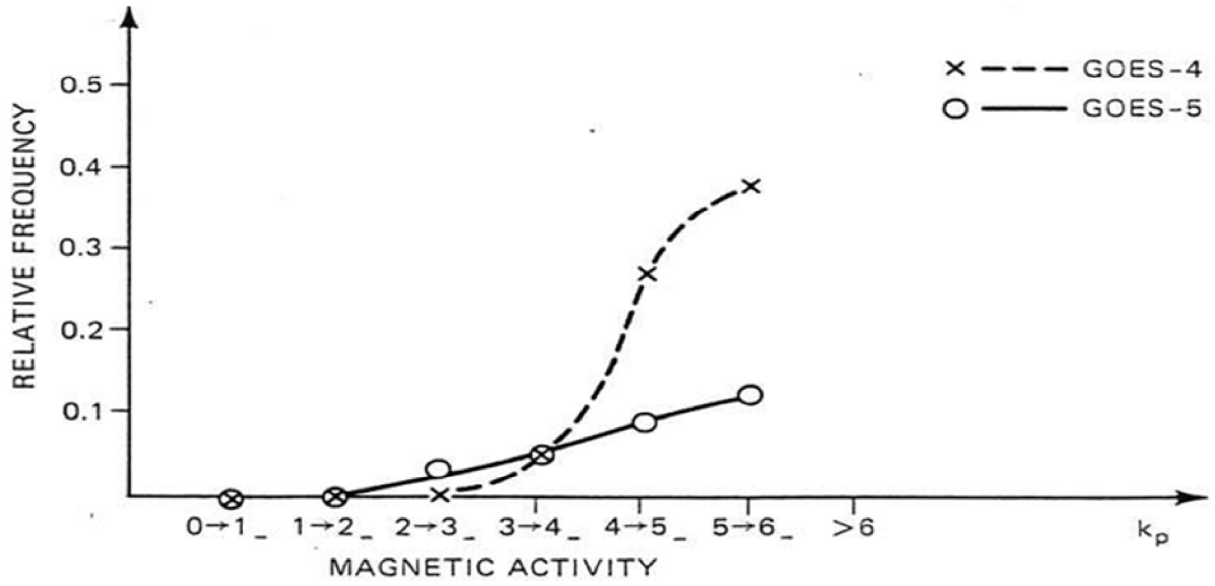

Fig. 16. Satellite anomaly occurrences vs magnetic activity for GOES-4 and GOES-5, with design changes made in GOES-5 using history of GOES-4.

Another case in point regarding design modification to improve mitigation of space weather effects on satellites concerns Anik-E1, Anik-E2, and Intelsat-K, which are three geostationary satellites of the same type. As mentioned earlier, the failures of Anik-E1 and Anik-E2 on January 20, 1994 wreaked havoc in communication across Canada, as the recoveries of the Anik-Es took considerable time [Lam et al., 2012]. Anik-E1 was restored to service within seven hours after the incident, and Anik-E2 took longer, requiring more than six months to have the full function back. Intelsat-K also wobbled on January 20, 1994, but recovered quickly. What made this interesting is that the Intelsat-K and the two Anik satellites are of the same satellite design (GE Astro Space 5000 (AS 5000)/Lockheed 5000). The crucial difference, however, is that the Intelsat Corporation specifically modified the design, thereby allowing the Intelsat-K satellite to resume operation quicker than the unmodified Anik-E satellites. Thus, this case and the previous example on GOES-4 and GOES-5 (Fig. 16) show that modification in engineering design to satellites of the same make can result in the reduction of space weather impacts on satellites.

Space Weather Consideration

Design consideration alone cannot ensure total immunity of satellites to space weather effects. When a severe space weather event of extreme intensity occurs, a satellite 'hardened' with thick shielding and ideal design may not be immune. Thus, forecast of space weather and situational awareness of the space environment have important roles to play in helping to minimize the susceptibility of satellites to space weather. NRCan Space Weather Group carries out work relevant to the mitigation of space weather effects on satellites. It operates the Canadian Space Weather Forecast Centre that dispenses forecasts to provide warning of pending high electron environment that could impact satellites.

Forecast of >2Mev energetic electrons that are the culprit of internal charging is available on NRCan's Canadian Space Weather Forecast Centre web site: http://www.spaceweather.gc.ca/sffl-eng.php. NRCan provides forecasts of energetic electron fluence (which is an accumulation over 24 hours of the electron fluxes) for up to 3 days. The forecasts are updated automatically every day at ~ 04 UT (around local midnight in Ottawa), and are based on the algorithms of Lam [2002] and Lam [2004]. A "screen shot" of the electron forecast web page is shown in Fig. 17. The plot in the "screen shot" shows forecasts (indicated by colored rectangles) of the fluence of highly energetic electrons with energies greater than 2 Mev at an altitude of 6.6 Earth radii in the geosynchronous orbit. The large black dots indicate observed fluence from the GOES-12 satellite, courtesy of NOAA's SWPC, for comparison with the forecasts. The horizontal dotted line in red is the "Threshold". The threshold value is based on the work of Wrenn and Smith [1996], and is the demarcation line between the fluence level that is safe for satellite and one that

could result in internal charging. Each colored rectangle indicates the range of the electron forecast values, and is green below the threshold. However, when it touches or is above the threshold, it turns red, which signals adverse space weather conditions hazardous to geosynchronous satellites. When this happens, there is a high likelihood of internal charging of satellite components by energetic electrons, with possible electric discharges that could result in malfunction or even complete failure of the satellite. NRCan's energetic electron forecast is thus able to give satellite operators 1-3 days warning time to take appropriate actions to mitigate the effects of internal charging such as putting staff on full alert status ready to respond instantly to problems, rescheduling important manoeuvres and delaying the dispatch of commands so as not to trigger a discharge that might cause an anomaly. A red rectangle that would appear above the "Threshold" in the electron forecast plot should alert satellite operators to be vigilant on possible internal charging, thus serving as an important guideline in the reduction of space weather impacts on satellites.

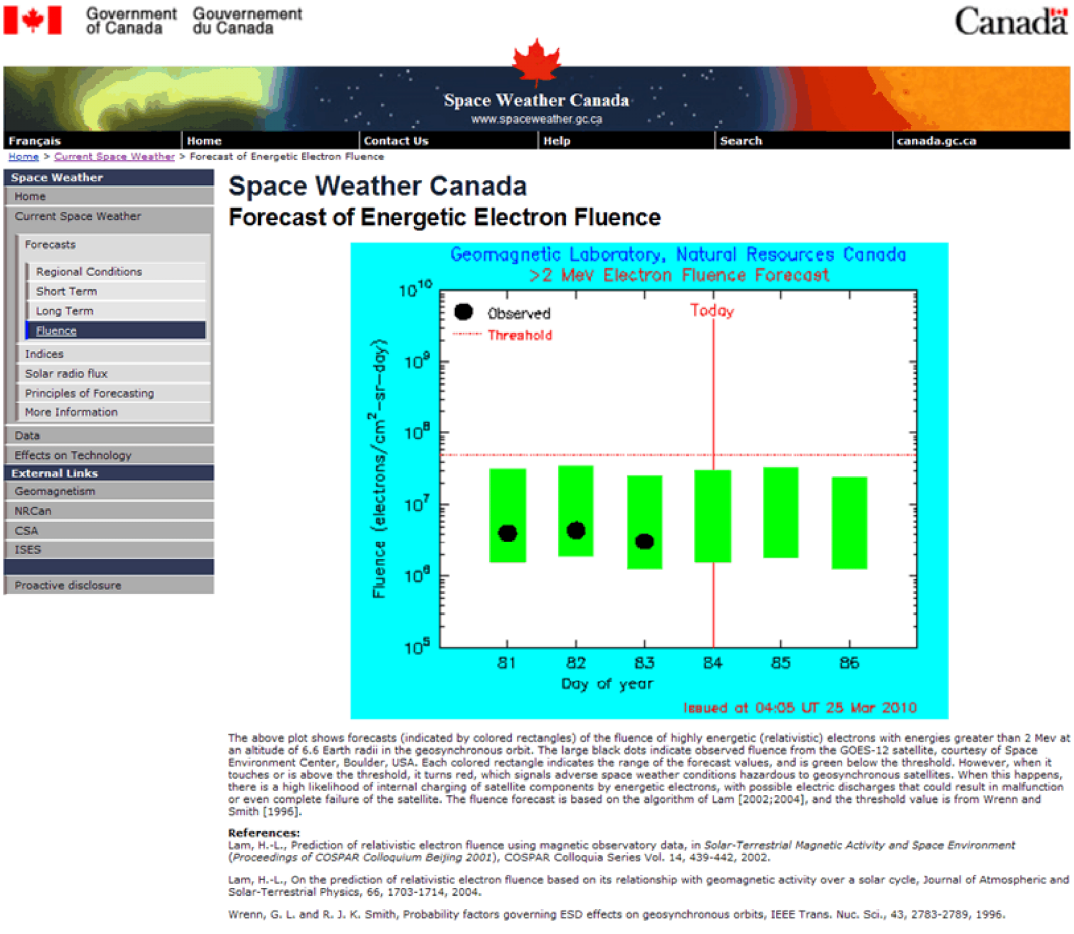

Fig. 17. “Screen shot” of NRCan’s energetic electron forecast web page.

In the early days when attention was paid to surface charging, Pike and Bunn [1976] reported that over 90 % of the satellite anomalies occurred during substorms. Thus, substorms can be considered as a good indicator of a space environment conducive to surface charging. While global geomagnetic storm can be forecast by noting time of occurrence of a solar eruption as well as its size, transit-time from Sun to Earth based on the speed of the eruption, and interplanetary conditions, it is not possible, given the current state of knowledge, to forecast the rather localized substorm due to sudden dynamical and explosive energy release from the magnetotail on the night side of the Earth. However, with a nation-wide distribution of magnetic observatories operated by NRCan's Geomagnetic Laboratory and its Space Weather Group's expertise in geomagnetic work, it is possible to stipulate some practical guidelines as one of the arsenals to help mitigating surface charging effects.

Fig. 18 is a stack plot of geomagnetic variations recorded by NRCan's magnetic observatories (http://suntwo.geomag.nrcan.gc.ca/under_construction/stackpull.html). It can be seen from the magnetic fluctuations that the magnetic trace's excursion sometimes resembles a bay on the coastline of a landmass. Since magnetic substorms are due to the intensification of the westward substorm electrojet, the negative bay in the X-component signifies the occurrence of substorm. For the auroral stations of IQA (Geographic coordinates: 63.7^0 N, 291.5^0 E; Geomagnetic coordinates: 74.4^0 N, 4.9^0 E), BLC (64.3^0 N, 263.9^0 E; 73.5^0 N, 320.7^0 E), and YKC (62.5^0 N, 245.5^0 E; 69.1^0 N, 297.9^0 E), the stack plot shows that substorm occurred in IQA first, then at BLC, and then at YKC. With IQA locating east of

BLC which, in turn, is located east of YKC, the occurrence of substorms in NRCan's eastern auroral zone station can be used as precursor to substorms that would occur later in a western auroral zone station. Thus, if the footprints of the field lines threading a geosynchronous satellite are in the vicinities of western auroral stations, the satellite operator can monitor the magnetic variations of eastern stations in real-time for signs of substorm and hence surface charging that may occur later.

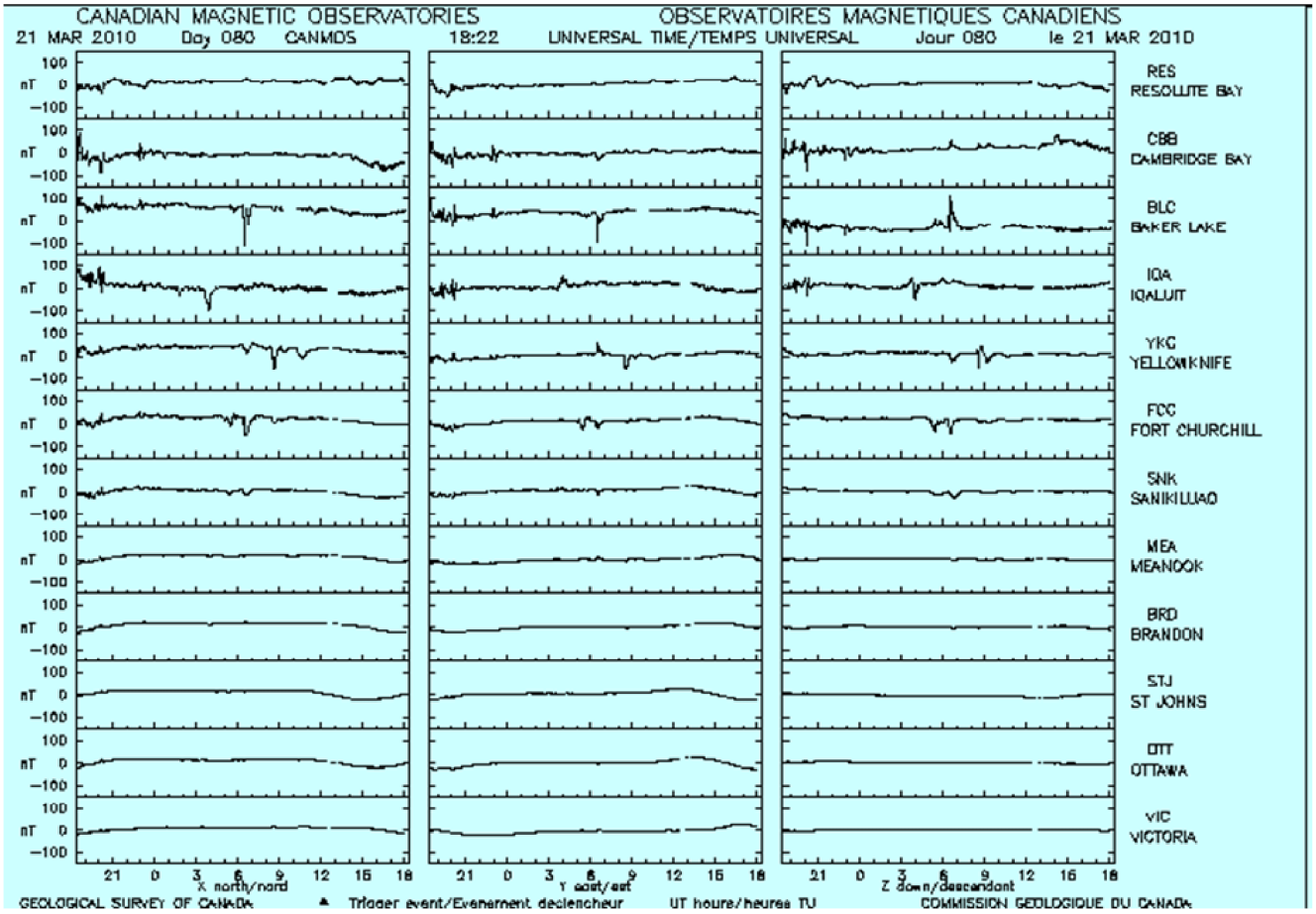

Fig. 18. A stack plot of magnetic variations recorded by NRCan's observatories.

However, the use of NRCan's eastern auroral zone stations as precursor to substorms that would occur later in western auroral zone stations depends on the location of the western substorm electrojet that varies from event to event. To illustrate this point, consider Fig. 19 which is a stack plot similar to Fig. 18 but shows simultaneous occurrence of substorms in the auroral zone stations. In Fig. 18 the negative bay at IQA occurred earlier than the one at BLC whereas in Fig. 19 the negative bays occurred at the same times at both IQA and BLC. Wiens and Rostoker [1975] showed steplike westward expansion of the westward substorm electroject with simultaneous onset of the electrojet in a given segment. Thus, Fig. 19 suggests that all the auroral stations were within a given segment of the substorm electroject, thus observing substorm occurrence simultaneously while Fig. 18 indicates two segments of the electroject with the first segment occurring at IQA first and the second segment occurring at BLC later. This should be kept in mind when using stack plots as a guide.

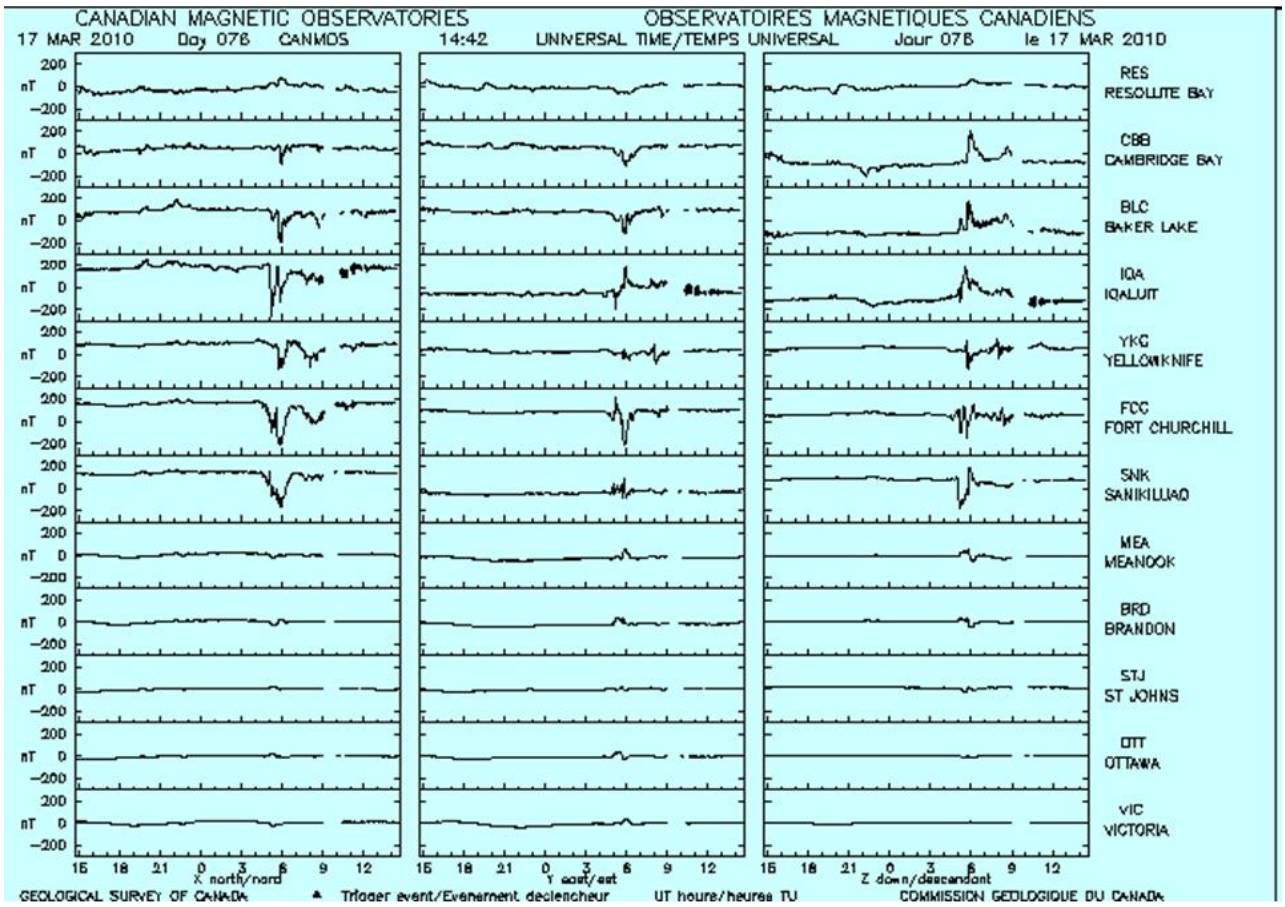

Fig. 19. A stack plot of magnetic variations recorded at NRCan's magnetic observatories.

It is sometimes difficult for a person without much experience in geomagnetic work to look at the wildly fluctuating traces of the magnetic variation to identify the occurrence of substorm. Recognizing this, Lam [2006] has formulated a simple index for nowcasting substorm. The index was derived based on the association of a certain kind of magnetospheric Ultra Low Frequency (ULF) waves, known as Pi2 pulsations, with substorm.

Pi2 pulsations are nighttime impulsive geomagnetic field fluctuations having irregular forms in the 6.7 - 25 mHz frequency band (corresponding to a 40 - 150 s period range). It was established long ago that these pulsations accompany geomagnetic bay onsets [Saito, 1961] and have maximum amplitudes in the auroral zone with close relation to the bay current systems [Jacobs and Sinno, 1960]. Pi2 pulsations were first used in a coordinated manner to identify substorm onsets by Rostoker [1968]. Since then, Pi2 has been considered to be a sensitive indicator of substorm onsets in substorm-related studies [e.g., Saito et al., 1976; Hsu and McPherron, 2003].

In addition to its role as a substorm onset identifier, Pi2 itself should also be a good proxy for a substorm because typical substorm magnetic bays contain a minimum of two Pi2 wave trains and often more, as also noted by Rostoker [1968]. However, these rather unique characteristics of Pi2 seem not to be fully utilized in space weather applications. Lam [2006] therefore sought to make use of these unique features of Pi2 to nowcast substorms by developing a simple Pi2 index, that can be easily generated in real-time to alert the occurrence of substorm for: power grid operators (worried about geomagnetically induced currents (GICs) caused by a substorm electrojet), nighttime aeromagnetic

surveyors (concerned about survey data exceeding a specific tolerance level because of substorm activities), the general public (interested in aurora due to precipitation of substorm particles), and satellite operators (concerned about spacecraft surface charging induced by inflow of substorm particles).

An example of Pi2 pulsations and substorm is shown in Fig. 20 (after Lam, 2006), showing substorm in the top panel and the associated Pi2 pulsations in the bottom panel recorded in PBQ (in auroral zone) and OTT (in subauroral zone). The negative bays in X due to the intensification of the westward substorm electrojet (located between PBQ and OTT as inferred from Z bays) signaled the occurrence of a magnetic substorm. The Pi2 pulsations, revealed after band-pass filtering the data, occurred in concert with the bay activities. A large Pi2 burst in the subauroral station of OTT at substorm onset is the classic substorm signature (at middle and low latitude), often used to identify substorm onsets at stations far away from the source region. After the initial bursts, a large Pi2 burst in the auroral station of PBQ is concomitant with the large excursion of the negative X bay, suggesting the contribution to the Pi2 spectrum by the electrojet. It is clear from the figure that magnetic substorm bays contain Pi2 wave trains and that Pi2 pulsations are a good proxy for magnetic substorms.

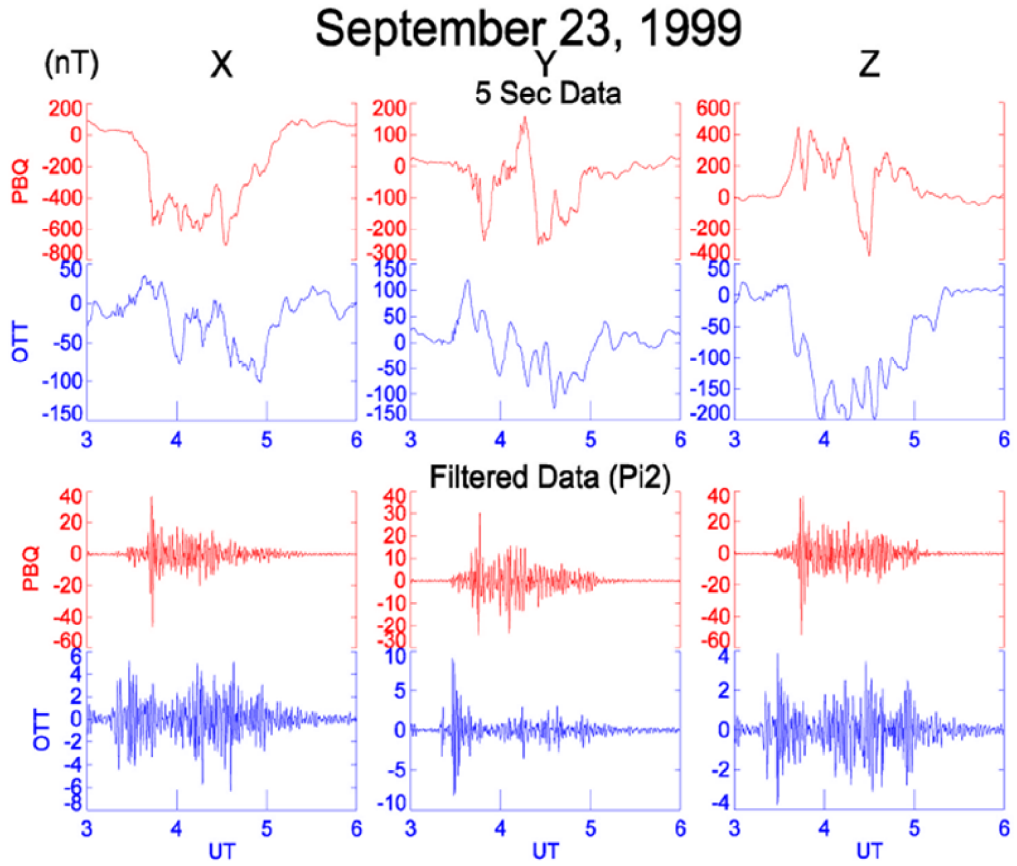

Fig. 20. Substorm (top) and Pi2 (bottom) observed at NRCan's magnetic observatories.

The simple Pi2 index, as devised by Lam [2006], has a simple and familiar scales of 0 - 9 used in the popular Kp or K geomagnetic indices. An example of the Pi2 index and substorm is shown in Fig. 21 (after Lam, 2006).

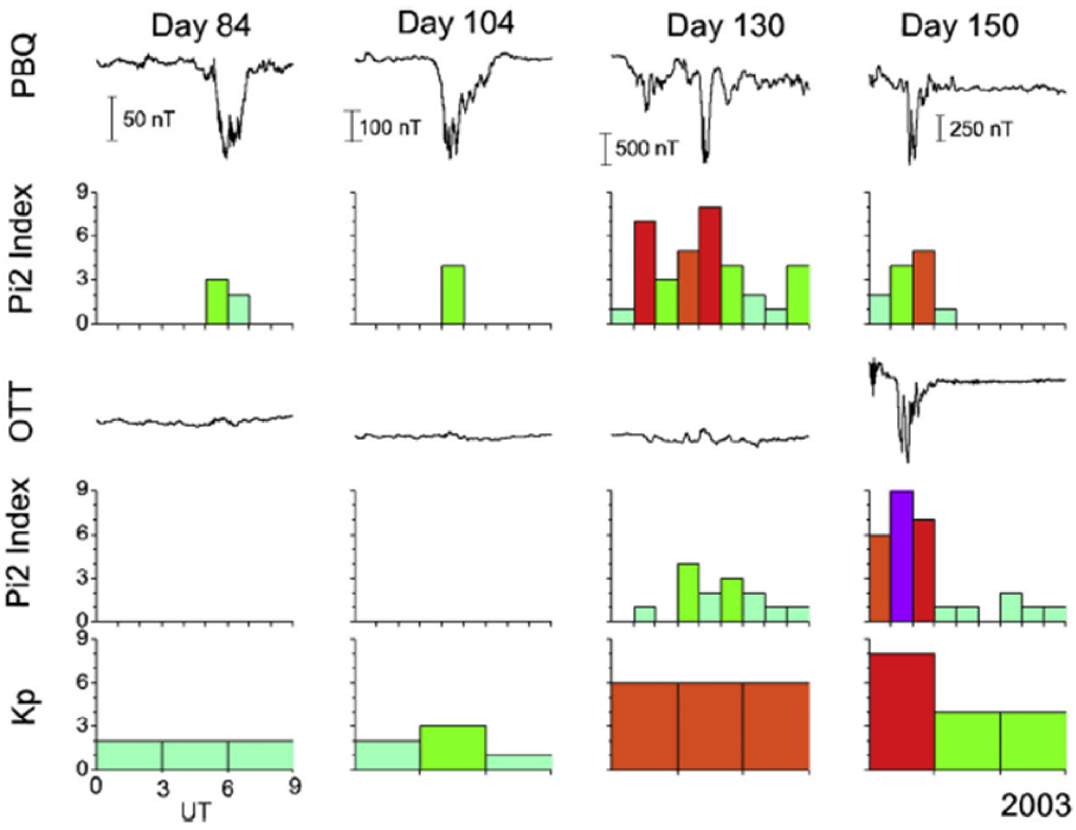

Fig. 21. Substorm and Pi2 index for four events in 2003, with Kp index at bottom for comparison.

It can be seen from Fig. 21 that the familiar Kp index does not denote any substorm, which is indicated by the negative bays in the magnetic traces, while the Pi2 index captures substorm occurrences quite well. If the value of the index is zero, there is no substorm. If the index attains a maximum value of 9, a severe substorm is on-going. Thus, by monitoring the simple values of the Pi2 index produced in real-time, satellite operators would know the occurrence of substorm and could take appropriate measures to mitigate the surface charging effects.

During substorms, streams of electrons are injected earthward from the magnetotail around local midnight and then drift eastward from midnight to dawn. Thus, if a satellite is located further from midnight toward dawn, the satellite would encounter the injection of particles later after the occurrence of a substorm. Using the relationship between the delay in the occurrence of anomalies after substorm onset and the local time of anomalies as shown in Fig. 22 (after Farthing et al., 1982), the time of occurrence of surface charging in a satellite located in the midnight to dawn sector can be estimated after a substorm has occurred. The slope on the plot corresponds to the drift time of 10 to 15 KeV electrons that were injected in the equatorial plane near midnight and then moved toward dawn under the influence of **V** x **B** forces. As the satellite is located further and further from midnight toward dawn, the delay from injection increases linearly.

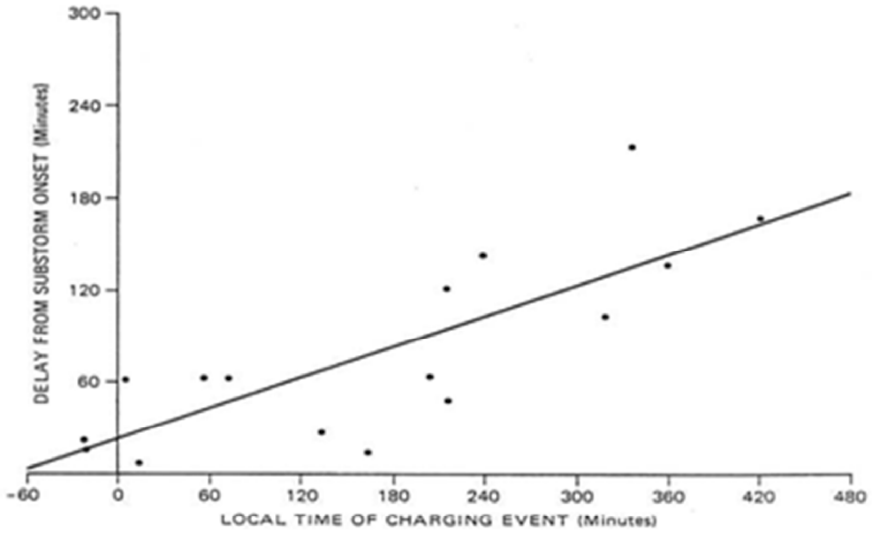

Fig. 22. Delay time after substorm onset vs local time of anomalies.

To surmise, guidelines regarding surface charging, hitherto not proposed before, using NRCan's geomagnetic resources are as follows: Situational awareness of the occurrence of substorm and hence surface charging can be gauged from real-time Pi2 index without the need to try to identify substorms on the magnetic traces. If a satellite is located in the midnight to dawn sector, it is possible to estimate the delay in surface charging after substorm onset using Fig. 22. If footprints of field lines threading the satellites are in the vicinities of auroral stations in the west, a substorm that is seen only in the east can be used as precursor for substorm in the west and hence charging that would occur later.

Arrivals of enhanced fluxes of energetic protons at geostationary orbit could result in single event upsets (SEUs) in satellites. However, there is currently no proton forecast service available at NRCan or at any other space weather forecasting centers elsewhere in the world. Nevertheless, NOAA's SWPC issues a proton event alert if energetic proton fluxes exceed a certain threshold. The proton event alerts are available online in http://www.swpc.noaa.gov/alerts/warnings_timeline.html, or can be notified by email through subscription to NOAA. Although a proton event alert is not a forecast, it can at least make the satellite operators aware of the current situation of a high proton environment, and can prompt them to be vigilant on possible SEUs.

Space Weather Anomaly Investigation System

A Space Weather Anomaly Investigation System (SWAIS) has been developed by NRCan Space Weather Group to gauge whether a satellite operational anomaly can be attributable to space weather, and, if so, the specific space weather condition that causes the anomaly. The system utilizes magnetic data from NRCan's magnetic observatory network, X-ray data, and particle data from the US GOES satellites. A stack plot summarizes magnetic variations, X-ray flux, and particle fluxes for protons with energies > 1, >10 and >100 MeV, as well as for electrons with energies > 0.6 and >2 MeV. Large negative bay type variations in the magnetic traces around local midnight observed by auroral stations threaded by field lines to geosynchronous distance signify occurrence of magnetic substorm, which may be proxy for surface charging. Large X-ray fluxes may give hints to solar array degradation and downlink problems. Large proton fluxes may be associated with single event upsets. Enhanced fluxes of electrons for an extended period of time may be telltale of internal charging. Thus, SWAIS provides a snap shot of the space weather conditions behind the occurrence of satellite anomalies. By bringing the relevant data conveniently together, SWAIS alleviates the efforts of satellite operators or other interested persons to search the different kind of data, find the right intervals, and display them after an anomaly event. SWAIS not only allows post-event investigations to be rapidly carried out but also facilitates the building of a data base to chronicle the type of space weather condition that is the culprit of certain type of anomaly for a particular satellite. The information can then be used for future design modification of satellites of the same make. As can be seen from Fig. 16 regarding GOES-4 and GOES-5, a design change based on the anomaly history shaped by SWAIS would help to reduce space weather

impacts on satellite of similar model.

An example of SWAIS is shown in Fig. 23, which shows magnetic, x-ray flux, and particle flux conditions associated with two satellite operational anomalies experienced by Eutelsat W5 and EchoStar2 satellites on June 17, 2008 and July 14, 2008 respectively. These two anomalies were mentioned in emails that circulated in the satellite anomaly community of satellite operators, military, government agencies, and academia. The SWAIS plots of Fig. 23 were produced to check the space weather conditions surrounding the anomalies, and distributed to the anomaly enthusiasts world-wide.

The Eutelsat W5 anomaly, as described by Satellite News Digest: “The satellite experienced an anomaly to part of its power generator subsystem during the night of 16 to 17 June 2008. Following the anomaly, an inquiry board was set up, which after extensive studies issued a ruling concerning the definitive loss of one of the satellite's two solar panels, caused by the malfunction of a drive motor. Eutelsat, in conjunction with experts from Thales Alenia Space, reconfigured the satellite to cope with the loss of onboard power, initially leading to four transponders being shut down. The incident also reduced the satellite's service life by about three years.”

The EchoStar 2 anomaly: "DISH Network said that ‘on July 14, 2008, our EchoStar 2 satellite experienced a substantial failure that appears to have rendered the satellite a total loss. EchoStar 2 had been operating from the 148 degree orbital location primarily as a back-up satellite, but had provided local network channel service to Alaska and six other small markets. All programming and other

services previously broadcast from EchoStar 2 were restored to Echostar 1, the primary satellite at the 148 degree location, within several hours after the failure. EchoStar 2, which was launched in September 1996, had a book value of approximately US $6.4 million as of June 30, 2008.' Lockheed Martin had earlier admitted that under certain environmental and operational conditions the LM-7000 series satellites can suffer complete failure."

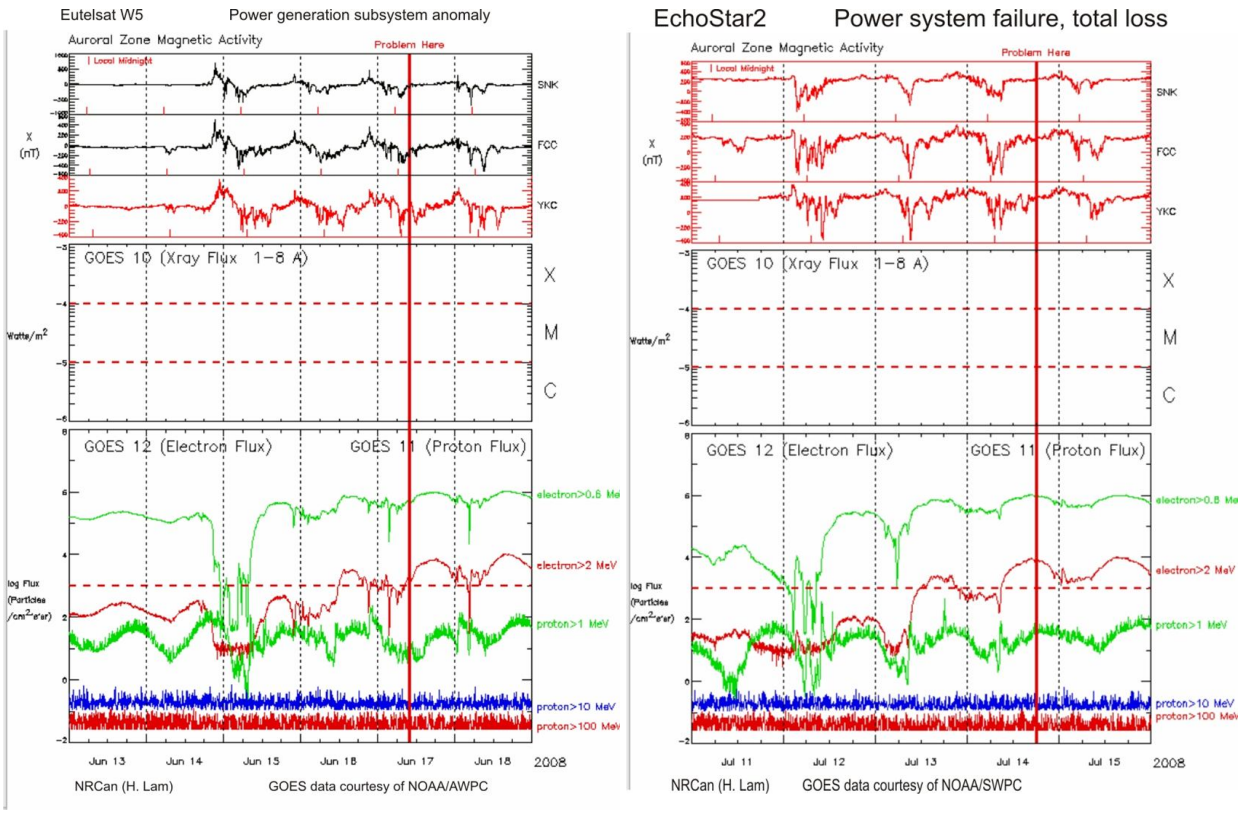

Fig. 23. Example of SWAIS for two satellite operational anomalies.

The top panel of each plot in Fig. 23 displays magnetic variations from NRCan's auroral magnetic observatories in proximities with footprints of field lines threading geosynchronous satellites at 6.6 R_E. Stations going from east to west are arranged from top to bottom so that the westward movement of the substorm electrojet can be easily seen. Since substorms occur in the midnight sector, local midnights for the stations are marked. Large negative excursions of the magnetic traces around local midnight signal the intensification of the substorm electrojet and the occurrence of substorm, indicating possible surface charging. The middle panel of X-ray flux plot indicate occurrences of flares above the C-flare threshold (i.e > 10^{-6} W m^{-2}). Satellite downlink problems may be due to interference from strong radio bursts that accompany large flares shown in this panel, which may also provide hints on solar array degradation due to solar flare protons. The bottom panel shows particle flux variations. Single event upsets (SEUs) may be associated with large proton fluxes. The proton event threshold is 10 protons/cm^2 - s- sr for protons with energies > 10 MeV. Internal charging may be associated with enhanced fluxes of electrons for an extended period of time, with the red dotted horizontal line set at 1E3 being the threshold for internal charging by electrons with energies > 2 MeV with electrostatic discharge possibility.

Based on the above guidelines, both the Eutelsat W5 anomaly and the EchoStar2 anomaly could be related to internal charging as suggested by the enhanced energetic electron flux above the threshold. Surface charging may also be the culprit for the Eutelsat anomaly, as suggested by the magnetic data. The low proton fluxes in both cases rule out single event upsets. The virtual absence of X-ray fluxes was in accordance with the minimum phase of the solar cycle that the anomalies were in.

Discussion

The NASA AE-8 and AP-8 models as well as the two NASA documents of NASA-TP-2361 and NASA-HDBK-4002 mentioned earlier are standards adhered to by the space community. However, there are other options available for design considerations. For long-term average electron fluxes in geostationary orbits, the new IGE-2006 average model [Sicard-Piet et al., 2008] presents another alternative. The IGE-2006 (International GEO electrons) model is based on two and a half solar cycles of in-orbit data coming from different space environment monitors which have been inter-calibrated. It provides the average and upper case electron flux at geostationary orbit for different energies (from 0.9 keV to 5.2 MeV) and for the eleven years around solar minimum. Also, new radiation specification models AP-9 and AE-9 for trapped radiation are being developed for satellite design specifications by the National Reconnaissance Office, the Aerospace Corporation, the Air Force Research Laboratory and Los Alamos National Laboratory [Byers et al., 2009].

For better definitions of worst-case scenarios in order to avoid space environment effects in satellite design, the FLUMIC (Flux Model for Internal Charging) model [Wrenn et al., 2000; Rogers et al., 2003] can be considered in evaluating severe internal charging environment. FLUMIC describes the electron flux, which has an exponential dependence on energy and varies with L-values (which are equatorial crossing distances of field lines, measured from the center of the Earth in R_e), time of year and phase of the solar cycle. There is also a software tool called DICTAT (DERA Internal Charging Threat Assessment Tool, with DERA referring to Defence Evaluation and Research Agency,

Farnborough, England) that enables spacecraft engineers to predict whether on-board dielectrics are vulnerable to electrostatic discharge [Rodgers and Levy, 1998]. The FLUMIC model used for internal charging assessments is integral to the DICTAT internal charging tool but can be applied separately. Both FLUMIC and DICTAT are available in European Space Agency (ESA)'s Space Environment Information System (SPENVIS) (http://www.spenvis.oma.be/spenvis/). Although the space community maybe reluctant to switch over to newer models because of the long history attached to the AE-8 and AP-8 models as well as the two NASA standards, alternative and newer tools such as those mentioned above allow further estimates of the radiation environment in design considerations for the mitigation of space weather impact on satellites regarding spacecraft charging.

For SEUs (single event upsets), the above models and guidelines are not applicable. Since SEUs are typically caused by high-energy ions which are 1,800 times more massive than electrons, these particles can pierce a spacecraft and its components, literally punching holes through them. SEUs usually involve changes to the memory of a satellite's computer circuits, sometimes locking up the electronic brain temporarily in the same way a terrestrial computer can crash. So, unless the satellite is 'hardened' by design to prevent the particle penetration, which is hard to accomplish because of weight consideration, there is not much a satellite operator can do upon receipt of space weather alert of proton events. They can only prepare for recovery from a failure rather than preventing one. For example, the onboard computer may be reset or computer systems may be reprogrammed from the ground.

For internal charging alerts using NRCan's energetic electron fluence forecast, it is worthwhile to

examine ‘how good’ the electron forecasts are. Fig. 24 (after Lam, 2004) shows a hindcast of electron fluence 2 days ahead (indicated in the figure as ‘Predicted Fluence’), observed electron fluence, and the occurrences of satellite anomalies in January 1994 when Anik-E1 and Anik-E2 malfunctioned. The figure shows that the postcast fluence tracks the observed fluence quite well, and the postcasts are all above the threshold of Wrenn and Smith [1996] for internal charging for the dates on which the anomalies occurred. Thus, if NRCan’s electron forecast service had been in place then, the satellite operators would have been forewarned of the high electron fluence ahead, and perhaps some actions could have been taken, such as putting a team on high alert, rescheduling important maneuvers and/or delaying the dispatch of commands so as not to trigger a discharge that might cause an anomaly.

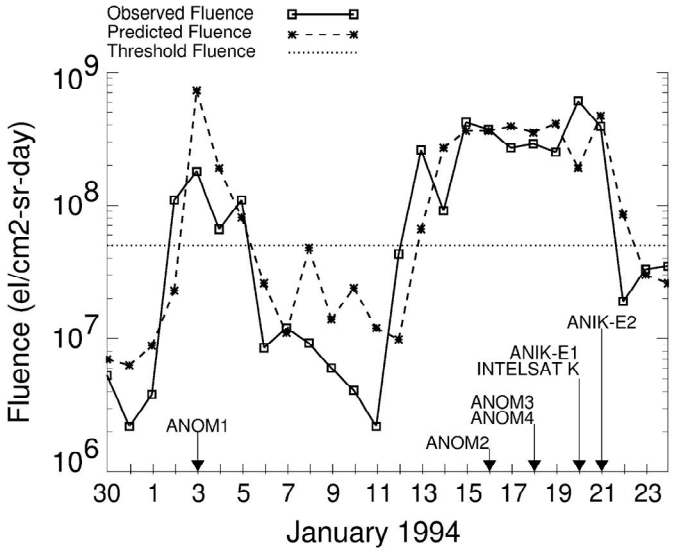

Fig.24. Observed fluence (solid line) and predicted fluence (dashed line) for January 1994 with dates of occurrences of satellite anomalies and threshold fluence level indicated.

To have a quantitative measure of 'how good' the electron forecasts are, scores were computed (see [Lam, 2006] for detail regarding the score computation). The scores vs years with Solar Cycle 23 superimposed are shown in Fig. 25 (after Lam, 2006).

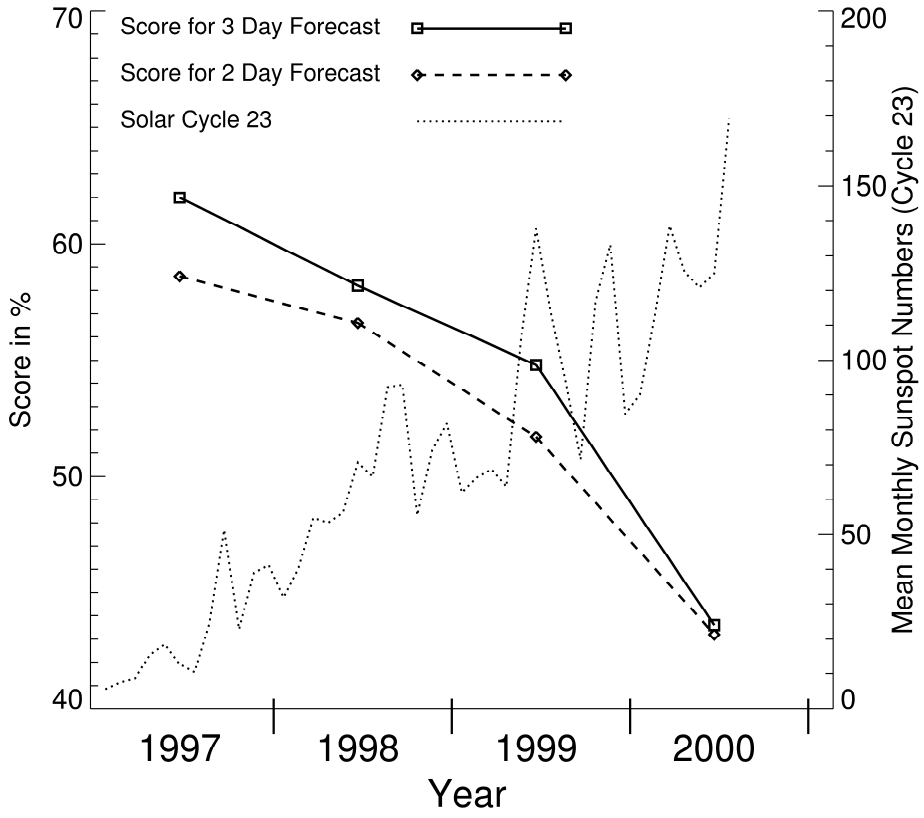

Fig. 25. Plot of electron forecast scores and sunspot number vs years.

It can be seen in Fig. 25 that scores decrease progressively from a high of 62% in 1997 towards a low of 43% in 2000 during the ascent of the solar cycle from minimum towards maximum. Thus, the algorithm currently in use does not perform well during solar maximum. Furthermore, the high score of 62% suggests that there is room for improvement in the prediction algorithm, although it should be pointed out the criterion for the computation of the score maybe a bit stringent. In day to day operation, it has been noticed that the trend of the forecast values follows the trend of the observed values quite well, even though both values may not exactly match. Hence, the electron forecasts, though not absolutely perfect, should be adequate for operational use by satellite operators, as a 1–3 day advance warning of dangerously high electron fluence is better than no warning at all. NRCan's electron forecast service must be performing a satisfactory service and is of value to the clients, as the web access statistics of hits of 5461, 6770, and 5367 for 2007, 2008, and 2009 respectively attest to.

In order to improve the forecast score, development of a better electron prediction algorithm is warranted so that days with dangerously high electron fluence are well forewarned 1-3 days in advance not only around solar minimum but also around solar maximum when the algorithm currently in use now appears to perform poorly according to the score of Fig. 25. The current NRCan electron forecast utilizes algorithms derived in Lam [2002] and Lam [2004], which are based on relationships between geomagnetic activity in terms of a daily magnetic index called DRX (a daily mean of the hourly ranges in the X-component (i.e. the northward component) of the geomagnetic variation recorded at an auroral zone station) and energetic electrons. A more refined analysis using high cadence of magnetic data may

lead to prediction improvement. Lam and Hruska [1991] pointed out earlier in their study of magnetic signatures of satellite anomalies that "analysis of links between pulsations and satellite anomalies might be a topic worth pursuing in the future". In particular, pulsations in the Pc5 band (1.7-6.7 mHz or 150-600 sec) have been invoked in Lam [2004] as an electron acceleration mechanism to explain Fig. 10, which shows high electron fluence during the descending phase of the solar cycle when recurrent coronal holes are prevalent. Coronal holes are sources of high-speed solar wind stream, which could excite large amplitude Pc5 pulsations through the action of the Kelvin Helmholtz instability along the magnetopause, according to the theoretical work of Chen and Hasagawa [1974]. Observationally, Engebretson et al. [1998] have shown that Pc5 pulsation power correlates well with solar wind speed. In addition, large amplitudes of Pc5 have also been observed to be associated with intensification of energetic electron flux over a 3-month period in 1994 in the declining phase of the solar cycle [Rostoker et al., 1998]. Pc5 as an accelerating mechanism for electrons has a solid theoretical grounding, as demonstrated by Liu et al. [1999]. Furthermore, recent work of Kim et al.[2006] indicates, albeit on event cases, the crucial role that strong Pc5 ULF waves plays as an acceleration mechanism for relativistic electrons under high-speed solar wind conditions that would not have resulted in enhanced relativistic electron fluxes had there been only weak ULF wave activities. Thus, evidence of enhancements of relativistic electrons by strong Pc5 ULF waves, which can be the acceleration mechanism for energizing seed electrons from a few hundred keV to relativistic energies of MeV, appears to be so strong that further work in this regard is clearly warranted.

A recent detailed re-examination of the Anik-E1 and Anik-E2 failures further proves that intense Pc5

activities were indeed associated with electron enhancements [Lam et al., 2012]. Fig. 26 shows such an association. The figure shows sonograms (i.e. the variations of power spectrums as a function of time) and the temporal variations of electron flux. Association of Pc5 ULF waves with enhanced fluxes (i.e. fluxes above the horizontal red line) can clearly be seen in the plots. Since magnetic pumping by ULF waves can lead to high energetic electron fluxes in a short time in terms of hours, the accelerating mechanism for electrons proposed in Liu et al. [1999] may be at work here. Thus, study of Pc5s with respect to energetic electrons at geosynchronous orbit should lead to an improved electron prediction algorithm.

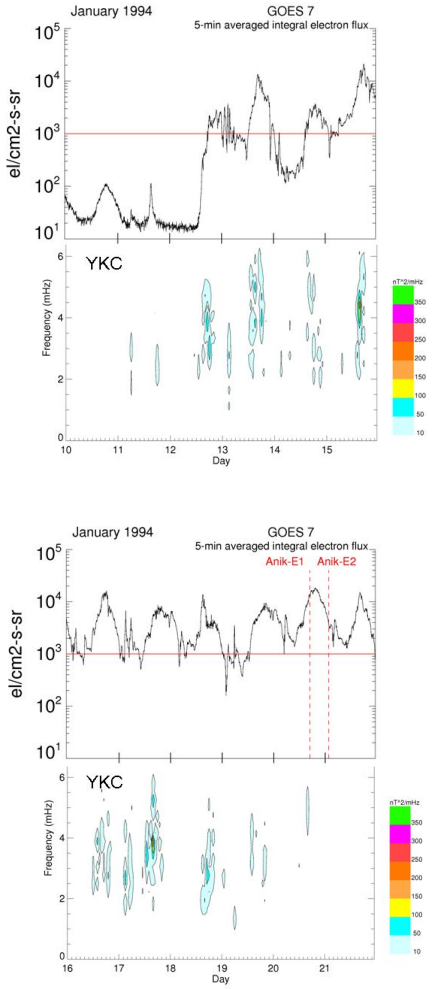

Fig. 26. Energetic electron flux (top panel) and sonogram (bottom panel) for January 10-15, 1994 (top figure) and January 16-21(bottom figure). Threshold for high electron flux (horizontal red line) and times of Anik-E failures (vertical red dashes) are indicated.

Charging is heavily dependent on the environment in a known fashion (i.e. substorm environment for surface charging and enhanced energetic electron environment for internal charging). However, knowing the occurrence of charging alone is not sufficient to mitigate the space weather impact on satellites because charge buildup on or in the satellite after prolonged high fluxes of electrons that can be predicted or nowcast is just the necessary condition for an anomaly. The sufficient condition would be conditions for a discharge that would result in the occurrence of the anomaly. Discharging may occur after charge buildup has reached a certain threshold. But it may also depend on spacecraft configuration, solar direction, and material parameter as demonstrated in the model study of Inouye [1976]. In addition, discharge may need to be triggered as shown by Wadham [1980], who noted the occurrences of cyclic charging and discharging on a metal lens barrel of an Earth sensor during revolution of the satellite from shadow to sunlight with discharging triggered by bombardment of photons in a photoelectric emission/surface discharge triggering mechanism. But, discharge trigger seems to be a subject of infrequent study. Thus, in re-investigating the space weather conditions that led to the Anik-E satellite outages, transient electromagnetic were examined to see if they could trigger discharging that disabled the Aniks. The result is shown in Fig. 27 (after Lam et al., 2012), which shows the magnetic conditions at times of satellite failures with conditions in geosynchronous altitude on top and those on the ground at the bottom. The figure shows that the Anik-E1 (111.1^0 W) failure occurred at a magnetic inflection at GOES-6 (112.6^0 W) and near the end of a pulsation train at YKC (114.5^0 W). Although the Anik-E2 (107.3^0 W) failure occurred after a magnetic inflection at GOES-6, the magnetic signature at YKC does not seem to be as clear. This is perhaps due to the footprint of Anik-E2 being further away from YKC than Anik-E1. In both cases, Hp (the north-south magnetic field vector) at GOES orbit

appeared to change sharply around the times of occurrences of the Anik E failures. Whether natural electromagnetic transients play a role as possible discharge triggers, as suggested by the Hp inflections associated with both satellite malfunctions and the ground pulsation trains associated with the Anik-E1 failure, is a subject worth pursuing in future studies of satellite operational anomalies.

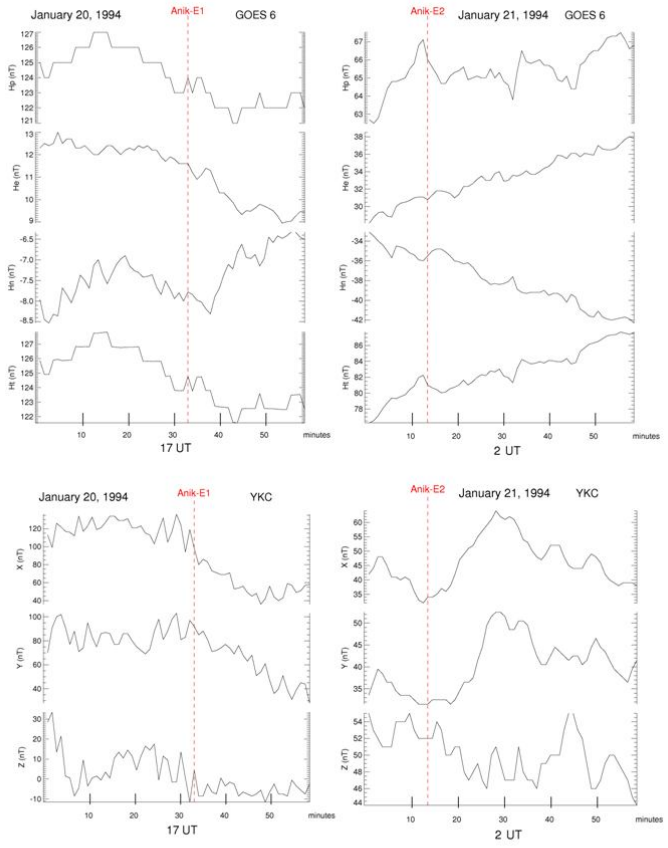

Fig. 27. Magnetic variations as observed by GOES-6 (top) and YKC (bottom) for January 20, 1994 for the hour of 17 UT (left) and for January 21 for the hour of 02UT (right).

Summary

Three of the major space weather effects on geostationary satellites and guidelines to reduce their impact have been presented. The three space weather effects are: (a) Single event upset (SEU) which is basically a "penetration" event in which high energy protons, or heavier ions enter a chip and "burn" a destructive track or deposit charge there; (b) Internal charging by > 2MeV energetic electrons due to dramatic increase in flux induced by high-speed solar wind streams mostly emanating from recurrent coronal holes that occur often during the descending phase of the solar cycle; (c) Surface charging by lower energy hot electrons due to sudden occurrence of explosive substorms in the midnight sector. The impacts on the satellites are: (a) The SEU changes the contents of chip memory, causes damage to stored data and to software, and may even render the CPU to halt, resulting in faulty commands. For (b) and (c), whether it is internal charging or differential surface charging, the charge buildup would produce an electric field that, after exceeding a certain threshold, could lead to an arc discharge, generating an electromagnetic transient that could couple into spacecraft electronics, causing a satellite operational anomaly or even a complete failure of the satellite.

To mitigate the space weather impacts on a satellite, the satellite can be 'hardened' by design. There are models and handbooks for such purpose. The standard NASA AE-8 as well as AP-8 models, and the newer IGE-2006 models, or the developing AE-9 and AP-9 models are available for radiation environment specifications that support engineering design. There are 2 NASA design guidelines to mitigate charging effects: (a) NASA-TP-2361 describes guidelines to avoid surface charging effects. (b)

NASA-HDBK-4002 describes guidelines to mitigate internal charging effects. Although the two standard NASA documents have become the primary design handbooks in their respective areas, there are other supplementary sources available, such as the FLUMIC model and the DICTAT tool of the Space Environment Information System of the European Space Agency.

Since the space environment surrounding geostationary satellites can vary with many orders of magnitude, it is not possible to render a satellite completely immune to space weather by design. A satellite may have been designed with a high degree of shielding, and with the right amount of ideal materials that can accumulate charge with charge leakage rate, and the sensitivity of the victim circuit taken into consideration. But, whether it can be protected from charging depends ultimately on the severity of the radiation environment. Thus, a timely warning and situational awareness of disturbed space weather conditions are necessary so that satellite operators can reschedule important manoeuvres, delay the dispatch of commands to avoid triggering a discharge, or go into a heightened state of alert by putting a team together ready to respond instantly to problems or to prepare for recovery for an impending dire situation. At NRCan, space weather forecast services are available to provide such warnings.

The Space Weather Group of NRCan provides energetic electron forecast that is updated daily to give a 1-3 days advance warning of internal charging due to high electron levels. Nowcasting of substorm by Pi2 index renders a situational awareness of surface charging. Warning of surface charging is possible by considering the precursory nature of substorms in the eastern magnetic stations, and the established

time-delay in anomaly occurrence in the midnight-dawn sector after substorm onset. The Space Weather Group has also developed the Space Weather Anomaly Investigation System (SWAIS) to relate space weather conditions to satellite problems due to surface charging, solar array degradation, downlink problems, internal charging, or single event upsets. Using SWAIS to find the culprit behind the anomaly and then to chronicle such events with anomaly records and environmental data would help to improve the design of satellites of similar make to prevent future recurrences.

References

Adams, J. H., Cosmic Ray Effects on Microelectronics Part 1: The Near-Earth Particle Environment, *NRL Report No. 4506*, 25 August 1982.

Allen, J. H., Satellite Anomalies, Recent Events, and Possible Causes, *SCOSTEP*, October 2000.

Allen, J. H., Historical and Recent Solar Activity and Geomagnetic Storms Affecting Spacecraft Operations, *Modern Space System Issues, GOMAC*, Monterey, California, March 2002.

Baker, D.N., Kanekal, S., Blake, J.B., Klecker, B., Rostoker, G., Lam, H.-L., Hruska, J., Anomalies on the ANIK communications spacecraft. *STEP International 4 (4)*, No. 4, *3–5, 1994.*

Byers, D., S. Huston, G. Ginet, T. P. O' Brien, T. Guild, D. Madden, and R. Friedel, AE/AP-9 Radiation Specification Model: An Update, *Space Weather Workshop*, Boulder, Apr 28- May 1, 2009.

Chen, L., Hasagawa, A., A theory of long period magnetic pulsations 1. Steady state excitation of field-line resonance, *Journal of Geophysical Research*, 79, 1024–1032, 1974.

DeForest, S. E., Spacecraft Charging at Synchronous Orbit, *Journal of Geophysical Research,* 77, 651-659, 1972.

Engebretson, M., Glassmeier, K.-H., Stellmacher, M., Hughes, W.J., Luhr, H., The dependence of high latitude Pc5 wave power on solar wind velocity and on the phase of high speed solar wind streams, *Journal of Geophysical Research*, 103, 26271–26283, 1998.

Farthing, W. H., J. P. Brown, and W. C. Bryant, Differential Spacecraft Charging on the Geostationary Operational Environmental Satellites, *NASA Technical Memorandum 93908,* March 1982.

Garrett, H. B., and Pike, C. P. (eds.), Space System and Their Interactions with Earth's Space Environment, *Progress in Astronautics and Aeronautics,* Vol. 71, MIT Press, Cambridge, MA, 1980.

Gubby, R., and Evans, J., Space Environment Effects and Satellite Design, *Journal of Atmospheric and Solar-Terrestrial Physics,* 64, 1723-1733, 2002.

Heppner, J. P., The Harang discontinuity in auroral belt ionospheric currents, *Geophysic Norvegica,* 29, 105-120, 1972.

Hsu, T.-S., and R. L. McPherron, Occurrence frequencies of IMF triggered and nontriggered substorms, *J. Geophys. Res.*, 108(A7), 1307, doi:10.1029/2002JA009442, 2003.

Inouye, G. T., Spacecraft potentials in substorm environment, in *Spacecraft Charging by Magnetospheric Plasma, Progress in Astronautics and Aeronautics,* Vol. 47, MIT Press, Cambridge, MA, 103-120, 1976.

Jacobs, J. A., and K. Sinno, World-wide Characteristics of Geomagnetic Micropulsations, *Geophysical Journal*, 3, 333 - 353, 1960.

Kim, H.-L., K. C. Kim, D.-Y. Lee, and G. Rostoker, Origin of geosynchronous relativistic electron events, *J. of Geophysical Research*, *111*, A03208, doi:10.1029/2005JA011469, 2006.

Kunstadter, C. T. W., Space Insurance: Perspectives and Outlook, *The First S-RAMP Conference,* Sapporo, Japan, October 2000.

Lam, H.-L., Prediction of relativistic electron fluence using magnetic observatory data, in Solar-Terrestrial Magnetic Activity and Space Environment (*Proceedings of COSPAR Colloquium Beijing 2001*), *COSPAR Colloquia Series,* Vol. 14, 439-442, 2002.

Lam, H.-L., On the prediction of relativistic electron fluence based on its relationship with geomagnetic activity over a solar cycle, *Journal of Atmospheric and Solar-Terrestrial Physics*, 66, 1703-1714, 2004.

Lam, H.-L., A simple index for Pi2 pulsations to nowcast substorms by Regional Warning Centre Canada, *Space Weather*, Vol. 4, S03001, doi:10.1029/2005SW000186, 2006.

Lam, H.-L., Hruska, J., Magnetic signatures for satellite anomalies, *Journal of Spacecraft and Rockets*, 28, 93–99, 1991.

Lam, H.-L., Boteler, D. H., Burlton, B., and Evans, J., Anik-E1 and E2 Satellite Failures of January 1994 Revisited, *Space Weather*, 10, S100003,doi:10.1029/2012SW000811, 2012.

Liu, W.W., Rostoker, G., Baker, D.N., Internal acceleration of relativistic electrons by large-amplitude ULF pulsations, *Journal of Geophysical Research*,104, 17391–17407, 1999.

Meulenberg, H., Jr., Evidence for a New Discharge Mechanism for Dielectric in a Plasma, *Spacecraft Charging by Magnetospheric Plasma, Progress in Astronautics and Aeronautics*, Vol. 47, MIT Press, Cambridge, MA, 237-246, 1976.

Mulville, D.R., Avoiding Problems Caused by Spacecraft On-Orbit Internal Charging Effects, *NASA-HDBK-4002*, 1999.

Purvis, C. K., Garrett, H. B., Whittlesey, A. C., and Stevens, N. J., Design Guidelines for Assessing and Controlling Spacecraft Charging Effects, *NASA-TP-2361*, 1984.

Pike, C. P., and Bunn, M. H., A Correlation Study Relating Spacecrafy Anomalies to Environmental Data, *Spacecraft Charging by Magnetospheric Plasma, Progress in Astronautics and Aeronautics*, Vol. 47, MIT Press, Cambridge, MA, 45-60, 1976.

Rodgers, D. J. and L. Levy, Engineering Tools for Internal Charging, *Space Environments and Effects*, ESTEC, Noordwijk, The Netherlands, September 15-16, 1998.

Rodgers, D. J., L. M. Murphy and C. S. Dyer, Benefits of a European Space Weather Programme, *DERA report no. DERA/KIS/SPACE/TR000349. ESWPS-DER-TN-0001*, Issue 2.1 December 19, 2000.

Rodgers D. J, Hunter K.A and Wrenn G.L, The Flumic Electron Environment Model, *Proceedings 8th Spacecraft Charging Technology Conference*, Huntsville Alabama, 2003.

Rosen, A. (ed.), Spacecraft Charging by Magnetospheric Plasma, *Progress in Astronautics and Aeronautics*, Vol. 47, MIT Press, Cambridge, MA, 1976.

Rostoker, G., Macrostructure of geomagnetic bays, *Journal of Geophysical Research*., 73, 4217 - 4229, 1968.

Rostoker, G., Skone, S., Baker, D.N., On the origin of relativistic electrons in the magnetosphere associated with some geomagnetic storms, *Geophysical Research Letters,* 25, 3701–3704, 1998.

Saito, T. (1961), Oscillation of geomagnetic field with the progress of pt-type pulsation, *Sci. Rep. Tohoku Univ., Ser. 5*, 13, 53 - 61, 1961.

Saito, T., K. Yumoto, and Y. Koyama (1976), Magnetic pulsation Pi2 as a sensitive indicator of magnetospheric substorm, *Planet. Space Sci.*, 24, 1025 - 1029, 1976.

Sawyer D.M. and J.I. Vette, AP-8 Trapped Proton Environment for Solar Maximum and Solar Minimum, *NSSDC WDC-A-R&S Report 76-06*, NASA-GSFC, 1976.

Sicard-Piet, A., S. A.Bourdarie, D. M. Boscher, R. H. W. Friedel, M. Thomsen, T. Goka, H.Matsumoto, and H. Koshiishi, A new international geostationary electron model: IGE-2006, from 1 keV to 5.2 MeV, *Space Weather*, 6, S07003, doi:10.1029/2007SW000368, 2008.

Steven, N. J., and Pike, C. P. (eds.), Space Charging Technology 1980, *NASA-CP-2182*, Air Force Geophysics Lab., TR-81-0270, 1981.

Vette J.I., The AE-8 Trapped Electron Model Environment, *NSSDC WDC-A-R&S Report 91-24*, NASA-GSFC, 1991.

Wadham, P. N., Operational experience with Anik A, *AIAA Paper 80-0549*, April 1980.

Wiens, R., and Rostoker, G., Characteristics of the Development of the Westward Electrojet During the Expansive Phase of Magnetospheric Substorms, *Journal of Geophysical Research*, 80, 2109-2128, 1975.

Wrenn, G. L., Conclusive Evidence for Internal Dielectric Charging Anomalies on Geosynchronous Communications Spacecraft, *Journal of Spacecraft and Reckets*, 32, 514-520, 1995.

Wrenn, G. L. and R. J. K. Smith, Probability factors governing ESD effects on geosynchronous orbits, *IEEE Trans. Nuc. Sci.*, 43, 2783-2789, 1996.

Wrenn, G. L., D. J. Rodgers, and P. Buehler, Modeling the Outer Belt Enhancements of Penetrating Electrons, *Journal of Spacecraft and Rockets,* 37, 408-415, 2000.